

UWThPh-1997-18
 DFTT 54/97
 IASSNS-AST 97/52
 hep-ph/9710209

BOUNDS ON LONG-BASELINE $\bar{\nu}_e \rightarrow \bar{\nu}_e$ AND $\bar{\nu}_\mu \rightarrow \bar{\nu}_e$ TRANSITION PROBABILITIES

S.M. Bilenky

*Joint Institute for Nuclear Research, Dubna, Russia, and
 Institute for Advanced Study, Princeton, N.J. 08540*

C. Giunti

*INFN, Sezione di Torino, and Dipartimento di Fisica Teorica, Università di Torino,
 Via P. Giuria 1, I-10125 Torino, Italy*

W. Grimus

*Institute for Theoretical Physics, University of Vienna,
 Boltzmannngasse 5, A-1090 Vienna, Austria*

Abstract

We discuss long-baseline neutrino oscillations in the framework of the two 4-neutrino schemes which can accommodate all existing neutrino oscillation data. Negative results of short-baseline reactor and accelerator experiments allow to obtain rather strong bounds on the long-baseline $\bar{\nu}_e \rightarrow \bar{\nu}_e$ and $\bar{\nu}_\mu \rightarrow \bar{\nu}_e$ transition probabilities. We consider in detail matter effects and show that the vacuum bounds are not substantially modified. We also comment on corresponding bounds in 3-neutrino scenarios.

14.60.Pq, 14.60.St

Typeset using REVTeX

I. INTRODUCTION

The problem of neutrino masses and mixing (see, for example, Refs. [1–4]) is the central issue of modern neutrino physics. A new stage in the investigation of this problem is represented by long-baseline (LBL) neutrino oscillation experiments: CHOOZ [5], Palo Verde [6], Kam-Land [7], K2K [8] (KEK–Super-Kamiokande), MINOS [9] (Fermilab–Soudan), ICARUS [10] (CERN–Gran Sasso). The major goal of these experiments is to reach the sensitivity of the “atmospheric neutrino range” $10^{-3} \div 10^{-2} \text{ eV}^2$ for the neutrino mass-squared difference.

Concerning reactor experiments, the first LBL experiment CHOOZ is taking data now, the Palo Verde LBL experiment will start later this year and the Kam-Land experiment is scheduled to start in the year 2000. The accelerator LBL experiment K2K is planned to begin taking data in the year 1999, whereas the MINOS and ICARUS experiments will start in the first years of the next millennium.

What implications for future LBL experiments can be inferred from the results of short-baseline (SBL) neutrino oscillation experiments and solar and atmospheric neutrino experiments? We will consider here this question in the framework of two models with four massive neutrinos that can accommodate all the existing data on neutrino oscillations.

The results of many neutrino oscillation experiments are presently available. Indications in favour of neutrino oscillations were found in solar neutrino experiments (Homestake [11], Kamiokande [12], GALLEX [13], SAGE [14] and Super-Kamiokande [15]), in atmospheric neutrino experiments (Kamiokande [16], IMB [17], Soudan [18] and Super-Kamiokande [19]) and in the LSND experiment [20]. The data of these experiments can be explained if there is neutrino mixing with the following values of neutrino mass-squared differences:

$$\Delta m_{\text{sun}}^2 \sim 10^{-10} \quad \text{or} \quad 10^{-5} \text{ eV}^2, \quad \Delta m_{\text{atm}}^2 \sim 10^{-3} \div 10^{-2} \text{ eV}^2, \quad \Delta m_{\text{LSND}}^2 \sim 1 \text{ eV}^2. \quad (1.1)$$

The two estimates of Δm_{sun}^2 refer to the vacuum oscillation solution [21] and the MSW solution [22,23], respectively, of the solar neutrino deficit. The estimate of Δm_{atm}^2 derives from the zenith angle variation of the atmospheric neutrino anomaly. It has so far only been observed by Kamiokande [16] and Super-Kamiokande [19]. From the analysis of the data of the LSND experiment and the negative results of other SBL experiments (the strongest limits are provided by the Bugey [24] and BNL E776 [25] experiments), it follows that

$$0.3 \lesssim \Delta m_{\text{LSND}}^2 \lesssim 2.2 \text{ eV}^2. \quad (1.2)$$

There are also data of many different reactor and accelerator short-baseline neutrino oscillation experiments in which no indication in favour of oscillations was found (see the reviews in Ref. [26]).

Three different scales of mass-squared differences require schemes with (at least) four massive neutrinos [27–30] (see, however, Refs. [31–33] for scenarios with three massive neutrinos and Ref. [34] for comments on these scenarios). In Refs. [29,30] all possible 4-neutrino mass spectra with the solar, atmospheric and LSND mass-squared difference scales were considered. It was shown that only two of these schemes are compatible with all the existing data. In these two schemes the four neutrino masses are divided into two pairs of close masses separated by a gap of the order of 1 eV, which gives $\Delta m_{\text{LSND}}^2 = \Delta m_{41}^2 \sim 1 \text{ eV}^2$:

$$(A) \quad \underbrace{m_1 < m_2}_{\text{atm}} \ll \underbrace{m_3 < m_4}_{\text{sun}} \quad \text{and} \quad (B) \quad \underbrace{m_1 < m_2}_{\text{sun}} \ll \underbrace{m_3 < m_4}_{\text{atm}}. \quad (1.3)$$

In scheme A, $\Delta m_{21}^2 \equiv \Delta m_{\text{atm}}^2$ is relevant for the explanation of the atmospheric neutrino anomaly and $\Delta m_{43}^2 \equiv \Delta m_{\text{sun}}^2$ is relevant for the suppression of solar ν_e 's. In scheme B, the rôles of Δm_{21}^2 and Δm_{43}^2 are reversed.

In the framework of the schemes (1.3), the probabilities of SBL transitions have the form [29]

$$P_{\nu_\alpha \rightarrow \nu_\beta}^{(\text{SBL})} = \frac{1}{2} A_{\alpha;\beta} \left(1 - \cos \frac{\Delta m^2 L}{2p} \right) \quad (\beta \neq \alpha), \quad (1.4)$$

$$P_{\nu_\alpha \rightarrow \nu_\alpha}^{(\text{SBL})} = 1 - \frac{1}{2} B_{\alpha;\alpha} \left(1 - \cos \frac{\Delta m^2 L}{2p} \right), \quad (1.5)$$

which are similar to the standard two-neutrino transition probabilities. From now on we use the notation $\Delta m^2 \equiv \Delta m_{41}^2 \equiv m_4^2 - m_1^2$ for the SBL mass-squared difference, L is the source–detector distance, p is the neutrino momentum and the oscillation amplitudes are given by

$$A_{\alpha;\beta} = 4 \left| \sum_{k=1,2} U_{\beta k} U_{\alpha k}^* \right|^2 = 4 \left| \sum_{k=3,4} U_{\beta k} U_{\alpha k}^* \right|^2, \quad (1.6)$$

$$\begin{aligned} B_{\alpha;\alpha} &= 4 \left(\sum_{k=1,2} |U_{\alpha k}|^2 \right) \left(1 - \sum_{k=1,2} |U_{\alpha k}|^2 \right) \\ &= 4 \left(\sum_{k=3,4} |U_{\alpha k}|^2 \right) \left(1 - \sum_{k=3,4} |U_{\alpha k}|^2 \right), \end{aligned} \quad (1.7)$$

where U is the unitary mixing matrix that connects flavour and sterile fields with the fields of neutrinos with definite masses:

$$\nu_{\alpha L} = \sum_{k=1}^4 U_{\alpha k} \nu_{kL} \quad (\alpha = e, \mu, \tau, s). \quad (1.8)$$

Eqs.(1.5) and (1.7) and SBL disappearance data lead to further information on the schemes A and B. From the exclusion plots obtained in the Bugey [24], CDHS [35] and CCFR [36] disappearance experiments, it follows that

$$B_{\alpha;\alpha} \leq B_{\alpha;\alpha}^0 \quad (\alpha = e, \mu). \quad (1.9)$$

The values of these upper bounds depend on Δm^2 . We have considered the range

$$10^{-1} \text{ eV}^2 \leq \Delta m^2 \leq 10^3 \text{ eV}^2. \quad (1.10)$$

In this range of Δm^2 the amplitude $B_{e;e}^0$ is small, whereas $B_{\mu;\mu}^0$ is small for $\Delta m^2 \gtrsim 0.3 \text{ eV}^2$.

Taking into account the results of solar and atmospheric neutrino experiments, for the elements of the mixing matrix we have the following bounds in the two schemes (1.3):

$$(A) \quad c_e \leq a_e^0, \quad c_\mu \geq 1 - a_\mu^0, \quad (1.11)$$

$$(B) \quad c_e \geq 1 - a_e^0, \quad c_\mu \leq a_\mu^0, \quad (1.12)$$

where

$$c_\alpha \equiv \sum_{k=1,2} |U_{\alpha k}|^2 \quad (1.13)$$

and

$$a_\alpha^0 = \frac{1}{2} \left(1 - \sqrt{1 - B_{\alpha;\alpha}^0} \right) \quad (\alpha = e, \mu). \quad (1.14)$$

The values of a_e^0 and a_μ^0 are given in Fig. 1 of Ref. [37] (one can see that $a_e^0 \lesssim 4 \times 10^{-2}$ for Δm^2 in the range (1.10) and $a_\mu^0 \lesssim 10^{-1}$ for $\Delta m^2 \gtrsim 0.5 \text{ eV}^2$).

In the following we will use also the bounds on the amplitude of $\bar{\nu}_\mu^{(-)} \rightarrow \bar{\nu}_e^{(-)}$ transition which can be obtained from exclusion plots of the BNL E734 [38], BNL E776 [25] and CCFR [39] appearance experiments. Thus, we can write

$$A_{\mu;e} \leq A_{\mu;e}^0, \quad (1.15)$$

where the value of $A_{\mu;e}^0$ corresponding to each value of Δm^2 can be obtained from the combination of these exclusion plots.

In this paper we will show that, in the framework of the two schemes (1.3), rather strong limits on the LBL $\bar{\nu}_e \rightarrow \bar{\nu}_e$ and $\bar{\nu}_\mu^{(-)} \rightarrow \bar{\nu}_e^{(-)}$ vacuum transition probabilities are obtained. The first of these channels will be investigated in the CHOOZ, Palo Verde and Kam-Land experiments and the second one by the K2K, MINOS and ICARUS collaborations. There are no similar limits on the probability of $\bar{\nu}_\mu^{(-)} \rightarrow \bar{\nu}_\mu^{(-)}$ and $\bar{\nu}_\mu^{(-)} \rightarrow \bar{\nu}_\tau^{(-)}$ oscillations.

Furthermore, we will consider in this paper the LBL transition probabilities of the $\bar{\nu}_e \rightarrow \bar{\nu}_e$ and $\bar{\nu}_\mu^{(-)} \rightarrow \bar{\nu}_e^{(-)}$ channels in the presence of matter. We will show that the vacuum bounds are not substantially modified by matter corrections.

Let us stress that the bounds on the LBL transition probabilities that we have obtained are general, but are heavily based on the existing neutrino oscillation data and in particular on the LSND data. If the LSND indications in favour of $\bar{\nu}_\mu \rightarrow \bar{\nu}_e$ oscillations will not be confirmed by the future experiments, these bounds will not be valid.

Future measurements by LBL experiments of $\bar{\nu}_e \rightarrow \bar{\nu}_e$ and/or $\bar{\nu}_\mu^{(-)} \rightarrow \bar{\nu}_e^{(-)}$ transition probabilities that violate the bound presented in this paper would allow to exclude the 4-neutrino schemes (1.3).

II. VACUUM BOUNDS FOR LBL NEUTRINO OSCILLATIONS

A. The case $\Delta m_{\text{sun}}^2 L/2p \ll 1$

In scheme A, the probabilities of $\nu_\alpha \rightarrow \nu_\beta$ and $\bar{\nu}_\alpha \rightarrow \bar{\nu}_\beta$ transitions in LBL experiments are given by

$$P_{\nu_\alpha \rightarrow \nu_\beta}^{(\text{LBL,A})} = \left| U_{\beta 1} U_{\alpha 1}^* + U_{\beta 2} U_{\alpha 2}^* \exp\left(-i \frac{\Delta m_{21}^2 L}{2p}\right) \right|^2 + \left| \sum_{k=3,4} U_{\beta k} U_{\alpha k}^* \right|^2, \quad (2.1)$$

$$P_{\bar{\nu}_\alpha \rightarrow \bar{\nu}_\beta}^{(\text{LBL,A})} = \left| U_{\beta 1}^* U_{\alpha 1} + U_{\beta 2}^* U_{\alpha 2} \exp\left(-i \frac{\Delta m_{21}^2 L}{2p}\right) \right|^2 + \left| \sum_{k=3,4} U_{\beta k}^* U_{\alpha k} \right|^2. \quad (2.2)$$

These LBL formulas are derived by taking into account the fact that – apart from Kam-Land with the MSW solution of the solar neutrino deficit (see next subsection) – in LBL experiments $\Delta m_{43}^2 L/2p \ll 1$ and dropping the terms proportional to the cosines of phases much larger than 2π (we have $\Delta m_{kj}^2 L/2p \gg 2\pi$ for $k = 3, 4$ and $j = 1, 2$), which do not contribute to the oscillation probabilities averaged over the neutrino energy spectrum. The transition probabilities in scheme B ensue from the expressions (2.1) and (2.2) with the change

$$1, 2 \leftrightarrow 3, 4. \quad (2.3)$$

Since scheme B emerges from scheme A by the substitution (2.3) and since we will derive bounds on the LBL oscillation probabilities $P_{\nu_\alpha \rightarrow \nu_\beta}^{(\text{LBL,A})}$ and $P_{\bar{\nu}_\alpha \rightarrow \bar{\nu}_\beta}^{(\text{LBL,B})}$ as functions of $A_{\alpha;\beta}$, c_α and c_β , it is evident that such bounds apply equally to both schemes A and B and to neutrinos and antineutrinos by virtue of the definitions (1.6) and (1.13). Consequently, when dealing with such bounds we will omit the superscripts A, B indicating the specific scheme.

To derive limits on the LBL oscillation probabilities which are given by the results of the SBL oscillation experiments we apply the Cauchy–Schwarz inequality. It implies for scheme A that

$$\left| \sum_{k=1,2} U_{\beta k} U_{\alpha k}^* \exp\left(-i \frac{\Delta m_{k1}^2 L}{2p}\right) \right|^2 \leq c_\alpha c_\beta. \quad (2.4)$$

Using this inequality and the definition (1.13) of c_α , we find from the LBL probabilities in Eqs.(2.1) and (2.2) that the survival probabilities $P_{\nu_\alpha \rightarrow \nu_\alpha}^{(\text{LBL})}$ and $P_{\bar{\nu}_\alpha \rightarrow \bar{\nu}_\alpha}^{(\text{LBL})}$ are bounded by

$$(1 - c_\alpha)^2 \leq P_{\nu_\alpha \rightarrow \nu_\alpha}^{(\text{LBL})} \leq c_\alpha^2 + (1 - c_\alpha)^2. \quad (2.5)$$

As explained before these bounds are scheme-independent. In order to obtain bounds on the LBL transition probabilities $P_{\nu_\alpha \rightarrow \nu_\beta}^{(\text{LBL})}$ and $P_{\bar{\nu}_\alpha \rightarrow \bar{\nu}_\beta}^{(\text{LBL})}$ with $\beta \neq \alpha$, we take into account the definition (1.6) of $A_{\alpha;\beta}$ and the inequality (2.4). When inserted into Eqs.(2.1) and (2.2) they imply

$$\frac{1}{4} A_{\alpha;\beta} \leq P_{\nu_\alpha \rightarrow \nu_\beta}^{(\text{LBL})} \leq c_\alpha c_\beta + \frac{1}{4} A_{\alpha;\beta}. \quad (2.6)$$

The bounds (2.5) and (2.6) are the basis of the following considerations for the different oscillation channels in LBL experiments.

The smallness of c_e in scheme A (see Eq.(1.11)) implies that the electron neutrino has a small mixing with the neutrinos whose mass-squared difference is responsible for the oscillations of atmospheric and LBL neutrinos (ν_1, ν_2 in scheme A). Hence, the probability of transitions of atmospheric and LBL electron neutrinos into other states is suppressed. Indeed, taking into account the constraint $c_e \leq a_e^0$, the lower bound on $P_{\bar{\nu}_e \rightarrow \bar{\nu}_e}^{(\text{LBL})}$ and the upper bounds on $P_{\nu_\mu \rightarrow \nu_e}^{(\text{LBL})}$ which we will derive are rather strict.

Let us discuss first the bounds on the LBL survival probability $P_{\bar{\nu}_e \rightarrow \bar{\nu}_e}^{(\text{LBL})}$. With the constraint (1.11) on c_e , Eq.(2.5) implies that in both schemes A and B

$$1 - P_{\nu_\mu \rightarrow \nu_e}^{(\text{LBL})} \leq a_e^0 (2 - a_e^0) . \quad (2.7)$$

The curve corresponding to this limit obtained from the 90% CL exclusion plot of the Bugey [24] experiment is shown in Fig. 1 (solid line). For comparison, the expected sensitivities of the LBL reactor neutrino experiments CHOOZ and Palo Verde are also shown in Fig. 1 by the dash-dotted and dash-dot-dotted vertical lines, respectively. These expected sensitivities with respect to $1 - P_{\bar{\nu}_e \rightarrow \bar{\nu}_e}^{(\text{LBL})}$ have been extracted by us from the figures presented in Refs. [5,6] showing the sensitivity of the respective experiments in the two-generation $\sin^2 2\vartheta - \delta m^2$ plane (here ϑ is the mixing angle and δm^2 is the mass-squared difference), using the fact that for high values of δm^2 each experiment is sensitive only to the averaged survival probability $P_{\bar{\nu}_e \rightarrow \bar{\nu}_e}^{(\text{LBL})} = 1 - \frac{1}{2} \sin^2 2\vartheta$. Thus, the vertical lines in Fig. 1 correspond to $\frac{1}{2} \sin^2 2\vartheta$ at high δm^2 in the figures presented in Refs. [5,6]. The case of the Kam-Land experiment will be discussed in sections II B and III.

Figure 1 shows that, in the framework of the two schemes (1.3) with four neutrinos, which allow to accommodate all the indications in favour of neutrino oscillations, the existing data put rather strong limits on the probability of LBL transitions of ν_e into other states (for $\Delta m^2 \gtrsim 3 \text{ eV}^2$ the upper bound for $1 - P_{\bar{\nu}_e \rightarrow \bar{\nu}_e}^{(\text{LBL})}$ is close to the border of the region of sensitivity of the CHOOZ experiment, whereas for $\Delta m^2 \lesssim 3 \text{ eV}^2$ it is much smaller).

The shadowed region in Fig. 1 corresponds to the range (1.2) of Δm^2 allowed at 90% CL by the results of the LSND and all the other SBL experiments. It can be seen that the LSND signal indicates an upper bound for $1 - P_{\bar{\nu}_e \rightarrow \bar{\nu}_e}^{(\text{LBL})}$ of about 5×10^{-2} , smaller than the expected sensitivities of the CHOOZ and Palo Verde experiments.

Let us stress that, in the framework of the schemes under consideration, the smallness of c_e is a consequence of the solar neutrino problem. Consider for example scheme A. The probability of solar neutrinos to survive is given by

$$P_{\nu_e \rightarrow \nu_e}^{(\text{sun,A})} = \sum_{k=1,2} |U_{ek}|^4 + \left(1 - \sum_{k=1,2} |U_{ek}|^2 \right)^2 P_{\nu_e \rightarrow \nu_e}^{(3;4)} , \quad (2.8)$$

where $P_{\nu_e \rightarrow \nu_e}^{(3;4)}$ is the survival probability due to the mixing of ν_e with ν_3 and ν_4 , depending on the small mass-squared difference Δm_{43}^2 . From the results of SBL reactor experiments it follows that the quantity $c_e \equiv \sum_{k=1,2} |U_{ek}|^2$ can be small or large (close to one). In order

to have the energy dependence of the survival probability $P_{\nu_e \rightarrow \nu_e}^{(\text{sun,A})}$ and the suppression of the flux of solar ν_e 's that are required for the explanation of the data of solar neutrino experiments, we must choose a small value of c_e . In this case, the survival probability of $\bar{\nu}_e$'s in LBL reactor experiments is close to one.

We want to emphasize that from the constraint on a_μ^0 in Eq.(1.11) and from Eq.(2.5) no non-trivial bound on the $\nu_\mu \rightarrow \nu_\mu^{(-)}$ survival probability can be derived.

Let us now discuss the bounds on $\nu_\mu \rightarrow \nu_e^{(-)}$ transitions in LBL accelerator experiments. We will compare these bounds with the expected sensitivities of the K2K [8], MINOS [9] and ICARUS [10] experiments. Taking into account the constraints (1.11) on c_e and (1.15) on $A_{\mu;e}$, Eq.(2.6) implies that in both schemes A and B

$$P_{\nu_\mu \rightarrow \nu_e}^{(\text{LBL})} \leq a_e^0 + \frac{1}{4} A_{\mu;e}^0 . \quad (2.9)$$

Conservation of probability and Eq.(2.5) lead to a further upper bound:

$$P_{\nu_\alpha \rightarrow \nu_\beta}^{(\text{LBL})} \leq 1 - P_{\nu_\alpha \rightarrow \nu_\alpha}^{(\text{LBL})} \leq c_\alpha (2 - c_\alpha) \quad (\alpha \neq \beta) . \quad (2.10)$$

In general $P_{\nu_\beta \rightarrow \nu_\alpha}^{(\text{LBL})}$ can be different from $P_{\nu_\alpha \rightarrow \nu_\beta}^{(\text{LBL})}$ (if CP is violated in the lepton sector), but conservation of probability gives the same upper bound as Eq.(2.10) for the opposite transition $\nu_\beta \rightarrow \nu_\alpha$:

$$P_{\nu_\beta \rightarrow \nu_\alpha}^{(\text{LBL})} \leq 1 - P_{\nu_\alpha \rightarrow \nu_\alpha}^{(\text{LBL})} \leq c_\alpha (2 - c_\alpha) \quad (\alpha \neq \beta) . \quad (2.11)$$

Finally, these two equations hold evidently also for antineutrinos. Thus from Eq.(2.11) and the constraint (1.11) on c_e we obtain

$$P_{\nu_\mu \rightarrow \nu_e}^{(\text{LBL})} \leq a_e^0 (2 - a_e^0) . \quad (2.12)$$

Numerically, this bound is better than the bound (2.9) for the SBL parameter $\Delta m^2 \lesssim 0.4 \text{ eV}^2$.

Combining Eqs.(2.9) and (2.12), we finally arrive at

$$P_{\nu_\mu \rightarrow \nu_e}^{(\text{LBL})} \leq \min \left(a_e^0 (2 - a_e^0) , a_e^0 + \frac{1}{4} A_{\mu;e}^0 \right) . \quad (2.13)$$

The curve corresponding to this limit obtained from the 90% CL exclusion plots of the Bugey [24] experiment for a_e^0 and of the BNL E734 [38], BNL E776 [25] and CCFR [39] experiments for $A_{\mu;e}^0$ is shown in Figs. 2 and 3 by the short-dashed line. For comparison, the expected sensitivities of the LBL accelerator neutrino experiments K2K [8], MINOS [9] and ICARUS [10] are also indicated (the dash-dotted vertical line in Fig. 2 and the dash-dotted and dash-dot-dotted vertical lines in Fig. 3, respectively). These sensitivities have been obtained from the figures presented in Refs. [8–10] showing the sensitivities of the respective experiments in the two-generation $\sin^2 2\vartheta - \delta m^2$ plane with the method explained in the context of LBL

reactor experiments. Note, however, that the short-dashed lines in Figs. 2 and 3 have to be corrected for matter effects. This will be done in the next section.¹

The shadowed areas in Figs. 2 and 3 represent the range (1.2). The LSND [20] experiment also supplies the lower bound in vacuum

$$\frac{1}{4} A_{\mu;e}^{\min} \leq P_{\bar{\nu}_\mu \rightarrow \bar{\nu}_e}^{(\text{LBL})} \quad (2.14)$$

where $A_{\mu;e}^{\min}$ is the minimal value of $A_{\mu;e}$ allowed at 90% CL by the LSND experiment. Evidently, $A_{\mu;e}^{\min}$ only exists for the range (1.2) and the function $\frac{1}{4} A_{\mu;e}^{\min}$ of Δm^2 is represented in Figs. 2 and 3 by the left edge of the darkly shadowed regions. These regions extend to the right until they reach the bound (2.13).

Figs. 2 and 3 show that, in the framework of the schemes under consideration, the sensitivities of the MINOS and ICARUS experiments are considerably better than the upper bound (2.13) for $P_{\bar{\nu}_\mu \rightarrow \bar{\nu}_e}^{(\text{LBL})}$. The sensitivity of the K2K experiment does not seem to be sufficient to reveal LBL $\bar{\nu}_\mu \rightarrow \bar{\nu}_e$ oscillations, but matter corrections soften the bound (2.13), as we will discuss quantitatively in the next section. It is interesting to observe the existence of the lower bound (2.14) on this transition probability that follows from the LSND results. However, this lower bound is valid only in the case of LBL neutrino oscillations in vacuum. The corrections due to the matter effects in LBL experiments make it disappear (see section III).

In vacuum, the right-hand side of Eq.(2.12) is at the same time an upper bound on $P_{\bar{\nu}_e \rightarrow \bar{\nu}_\tau}^{(\text{LBL})}$. This is evident from Eq.(2.10). The bound (2.12) is quite prone to matter effects. On the other hand, the probability of $\bar{\nu}_\mu \rightarrow \bar{\nu}_\tau$ transitions is not constrained by the results of SBL experiments.

Finally, a further upper bound on $P_{\bar{\nu}_\alpha \rightarrow \bar{\nu}_\beta}^{(\text{LBL})}$ for $\alpha \neq \beta$ is gained from Eq.(2.6). Since $A_{\alpha;\beta} \leq 4(1 - c_\alpha)(1 - c_\beta)$, we have

$$P_{\bar{\nu}_\alpha \rightarrow \bar{\nu}_\beta}^{(\text{LBL})} \leq c_\alpha c_\beta + (1 - c_\alpha)(1 - c_\beta) \quad (\alpha \neq \beta). \quad (2.15)$$

Obviously, if $c_\alpha = c_\beta = 0$ or 1 is in the allowed range of these quantities, then this upper bound is 1 and thus is trivial. This leaves only $\alpha = \mu$ and $\beta = e$ as a non-trivial case, with

$$P_{\bar{\nu}_\mu \rightarrow \bar{\nu}_e}^{(\text{LBL})} \leq a_e^0 + a_\mu^0 - 2a_e^0 a_\mu^0. \quad (2.16)$$

The dotted curves in Figs. 2 and 3 show this limit with a_e^0 and a_μ^0 obtained from the 90% CL exclusion plots of the Bugey [24] $\bar{\nu}_e \rightarrow \bar{\nu}_e$ experiment and of the CDHS [35] and CCFR [36] $\nu_\mu \rightarrow \nu_\mu$ experiments, respectively. For $a_\mu^0 \ll a_e^0 \ll 1$ this bound is about half of that

¹The short-dashed lines in both figures are identical, however, they receive different matter corrections for K2K on the one hand and MINOS and ICARUS on the other hand. This will become clear in the next section.

given by Eq.(2.12). However, since a_μ^0 is only small in the same range of Δm^2 where $A_{\mu;e}^0$ is small, numerically the bound (2.16), which is stable against matter effects, turns out to be worse than the bound (2.9) in its matter-corrected form (see section III).

B. The case $\Delta m_{\text{sun}}^2 L/2p \sim 1$

If the MSW effect is responsible for the solar neutrino deficit the phase

$$\eta \equiv \frac{\Delta m_{\text{sun}}^2 L}{2p} \quad (2.17)$$

is not necessarily negligible in LBL reactor experiments. Indeed, we have

$$\eta \simeq 2.5 \times 10^{-2} \left(\frac{L}{1\text{km}} \right) \quad (2.18)$$

for $\Delta m_{\text{sun}}^2 \simeq 10^{-5} \text{eV}^2$ and $p \simeq 1\text{MeV}$. Hence, the phase η is negligible in the CHOOZ and Palo Verde experiments, which have a baseline of about 1 km, but is not negligible in the Kam-Land experiment, which has a baseline of about 150 km. From Eqs.(2.17) and (2.18) one can see that the phase η is a function of neutrino energy and is of order 1 for Kam-Land. For a vacuum oscillation solution of the solar neutrino deficit the corresponding phase is always negligible in LBL experiments.

In order to derive a bound on the survival probability $P_{\bar{\nu}_e \rightarrow \bar{\nu}_e}^{(\text{LBL})}$, it is convenient to write it (in scheme A) as

$$P_{\bar{\nu}_e \rightarrow \bar{\nu}_e}^{(\text{LBL,A})} = \left| |U_{e1}|^2 + |U_{e2}|^2 \exp \left(-i \frac{\Delta m_{21}^2 L}{2p} \right) \right|^2 + (|U_{e3}|^2 + |U_{e4}|^2)^2 - 2|U_{e3}|^2 |U_{e4}|^2 (1 - \cos \eta) . \quad (2.19)$$

It is clear that this probability is bounded from below by

$$P_{\bar{\nu}_e \rightarrow \bar{\nu}_e}^{(\text{LBL,A})} \geq (1 - c_e)^2 - 2|U_{e3}|^2 |U_{e4}|^2 (1 - \cos \eta) \geq (1 - c_e)^2 \cos^2 \frac{\eta}{2}, \quad (2.20)$$

where we have used the definition of c_e given in Eq.(1.13). Taking into account the constraint (1.11) on c_e , we obtain

$$1 - P_{\bar{\nu}_e \rightarrow \bar{\nu}_e}^{(\text{LBL})} \leq 1 - \cos^2 \frac{\eta}{2} (1 - a_e^0)^2 . \quad (2.21)$$

In the case of a small mixing MSW solution of the solar neutrino problem, either $|U_{e3}|^2$ or $|U_{e4}|^2$ is very small and the contribution of the term $2|U_{e3}|^2 |U_{e4}|^2 (1 - \cos \eta)$ in Eq.(2.19) is negligible. Hence, in this case the vacuum bound (2.7) on $1 - P_{\bar{\nu}_e \rightarrow \bar{\nu}_e}^{(\text{LBL})}$ is valid for all reactor LBL experiments, including Kam-Land. This bound is represented by the short-dashed line in Fig. 4 for the Kam-Land experiment.

In the case of a large mixing MSW solution, the contribution of the term $2|U_{e3}|^2|U_{e4}|^2(1 - \cos \eta)$ in Eq.(2.19) is not negligible. It is evident from Eq.(2.17) that the bound (2.21) depends on the neutrino energy. For example, assuming $\Delta m_{\text{sun}}^2 \simeq 10^{-5} \text{ eV}^2$, for $p = 2, 4, 7 \text{ MeV}$ we have, respectively, $\eta \simeq 1.9, 0.95, 0.54$ and $\cos^2 \frac{\eta}{2} \simeq 0.34, 0.79, 0.93$ in Kam-Land. The bounds derived with Eq.(2.21) corresponding to these neutrino momenta are represented by the dotted, dash-dotted and dash-dot-dotted lines in Fig. 4 for the Kam-Land experiment. One can see that for neutrino energies around 2 MeV the upper bound for $1 - P_{\bar{\nu}_e \rightarrow \bar{\nu}_e}^{(\text{LBL})}$ in Kam-Land practically disappears. Hence a measurement of a large transition probability $1 - P_{\bar{\nu}_e \rightarrow \bar{\nu}_e}^{(\text{LBL})}$ in the Kam-Land experiment at neutrino energies around 2 MeV and a suppression of the same probability at neutrino energies bigger than about 4 MeV would be an indirect indication in favour of the large mixing angle MSW solution of the solar neutrino problem.

If a large mixing MSW solution of the solar neutrino deficit is realized in nature, the value of Δm_{sun}^2 could be determined by an experiment like Kam-Land, having a sufficient neutrino energy resolution. Considering Eq.(2.19) and neglecting the first term on the right-hand side which is suppressed by $(a_e^0)^2$ we obtain

$$P_{\bar{\nu}_e \rightarrow \bar{\nu}_e}^{(\text{LBL,A})} \simeq (1 - c_e)^2 - 4|U_{e3}|^2|U_{e4}|^2 \sin^2 \frac{\eta}{2}. \quad (2.22)$$

As a function of p this survival probability has maxima at

$$p_0 = \frac{\Delta m_{\text{sun}}^2 L}{2\pi(2k + 1)} \quad (k = 0, 1, 2, \dots). \quad (2.23)$$

A measurement of these maxima would allow the determination of Δm_{sun}^2 .

III. MATTER CORRECTIONS

In this section we will derive the expressions for the LBL transitions in matter in the schemes (1.3) with mixing of four neutrinos. These schemes contain active and sterile neutrinos. In such a case, in the effective Hamiltonian of the interaction of neutrinos with matter there is an additional neutral current term apart from the usual charged current term. For the total Hamiltonians of neutrinos and antineutrinos we have the following expressions in the flavour representation [22]:

$$H_\nu = \frac{1}{2p} \left(U \hat{M}^2 U^\dagger + \text{diag} (a_{CC}, 0, 0, a_{NC}) \right), \quad (3.1)$$

$$H_{\bar{\nu}} = \frac{1}{2p} \left(U^* \hat{M}^2 U^T - \text{diag} (a_{CC}, 0, 0, a_{NC}) \right). \quad (3.2)$$

Here we have defined

$$a_{CC} = 2\sqrt{2} G_F N_e p \simeq 2.3 \times 10^{-4} \text{ eV}^2 \left(\frac{\rho}{3 \text{ g cm}^{-3}} \right) \left(\frac{p}{1 \text{ GeV}} \right), \quad (3.3)$$

$$a_{NC} = \sqrt{2} G_F N_n p \simeq \frac{1}{2} a_{CC}, \quad (3.4)$$

\hat{M}^2 denotes the diagonal matrix of the squares of the neutrino masses, G_F is the Fermi constant, N_e and N_n are the electron and neutron number density, respectively, and ρ is the density of matter, which in the Earth's crust is on average 3 g cm^{-3} . Since the lithosphere consists mainly of elements where the neutron number equals the proton number, we have $N_e \simeq N_n \simeq \frac{N_A \rho}{2 \text{ 1g}}$, where N_A is the Avogadro number. The parameters a_{CC} and a_{NC} can be as large as Δm_{atm}^2 , which is relevant for LBL oscillations. Their effects on the bounds for transition probabilities in LBL experiments need not be negligible, as we shall see.

In order to assess the size of matter effects, we consider the simplifying approximation of constant N_e and N_n , which is rather good in the case of LBL experiments. Furthermore, in the following we will concentrate on the scheme A and we will consider only the neutrino Hamiltonian (3.1). At the end of this section we will see that, as in the vacuum case, the bounds obtained for neutrinos in the scheme A are also valid for antineutrinos in scheme A and for neutrinos and antineutrinos in scheme B.

In order to obtain the expressions for the transition probabilities of neutrinos in matter, we have to diagonalize the Hamiltonian (3.1). With the diagonalization matrix U' we have

$$H_\nu = U' \frac{\hat{\epsilon}}{2p} U'^\dagger \quad (3.5)$$

where $\hat{\epsilon} = \text{diag}(\epsilon_1, \dots, \epsilon_4)$ and $U'^\dagger U' = \mathbf{1}$. Note that in the vacuum case $U' = U$ and $\epsilon_j = m_j^2$ ($j = 1, \dots, 4$). It is convenient to use the basis where $H_0 \equiv H_\nu(a_{CC} = a_{NC} = 0)$ is diagonal. In this basis we have

$$\hat{H}_\nu \equiv U^\dagger H_\nu U = \frac{1}{2p} \left(\hat{M}^2 + U^\dagger \text{diag}(a_{CC}, 0, 0, a_{NC}) U \right) = \frac{1}{2p} R \hat{\epsilon} R^\dagger \quad (3.6)$$

and the unitary matrix U' is given by

$$U' = UR. \quad (3.7)$$

Since $a_{CC} \ll \Delta m^2$, where $\Delta m^2 \equiv m_4^2 - m_1^2 \sim 1 \text{ eV}^2$ is relevant for SBL oscillations, it is obvious that, apart from corrections of order $a_{CC}/\Delta m^2$, the matrix R has the block structure

$$R = \begin{pmatrix} R_{\text{atm}} & 0 \\ 0 & R_{\text{sun}} \end{pmatrix}, \quad (3.8)$$

where R_{atm} and R_{sun} are 2×2 unitary matrices. All our considerations in this paper are based on this approximation. A glance at Tab. I shows that the ratio $a_{CC}/\Delta m^2$ is less than 10^{-2} for all the LBL experiments of the first generation. The block structure of R has the consequence that

$$\sum_{j=1,2} U'_{\alpha j} U'^*_{\beta j} = \sum_{j=1,2} U_{\alpha j} U^*_{\beta j} \quad (3.9)$$

and therefore

$$c_\alpha = \sum_{j=1,2} |U_{\alpha j}|^2 = \sum_{j=1,2} |U'_{\alpha j}|^2. \quad (3.10)$$

It is easy to calculate the energy eigenvalues up to terms of order $a_{CC}/\Delta m^2$. We are interested in the differences $\epsilon_2 - \epsilon_1$ and $\epsilon_4 - \epsilon_3$. Defining

$$|U_{\alpha 1}|^2 = c_\alpha \cos^2 \gamma_\alpha \quad \text{and} \quad |U_{\alpha 2}|^2 = c_\alpha \sin^2 \gamma_\alpha \quad \text{for} \quad \alpha = e, s \quad (3.11)$$

and

$$\delta = \arg(U_{e1}U_{e2}^*U_{s1}^*U_{s2}), \quad y_e = \frac{a_{CC}c_e}{\Delta m_{21}^2}, \quad y_s = \frac{a_{NC}c_s}{\Delta m_{21}^2} \quad (3.12)$$

we obtain for the atmospheric neutrino sector

$$\epsilon_2 - \epsilon_1 = \Delta m_{21}^2 \left[\left| 1 - y_e e^{2i\gamma_e} - y_s e^{2i\gamma_s} \right|^2 - 4y_e y_s \sin 2\gamma_e \sin 2\gamma_s \sin^2 \frac{\delta}{2} \right]^{1/2}. \quad (3.13)$$

Similarly, with

$$|U_{\alpha 3}|^2 = (1 - c_\alpha) \cos^2 \gamma'_\alpha \quad \text{and} \quad |U_{\alpha 4}|^2 = (1 - c_\alpha) \sin^2 \gamma'_\alpha \quad \text{for} \quad \alpha = e, s \quad (3.14)$$

and

$$\delta' = \arg(U_{e3}U_{e4}^*U_{s3}^*U_{s4}), \quad y'_e = \frac{a_{CC}(1 - c_e)}{\Delta m_{43}^2}, \quad y'_s = \frac{a_{NC}(1 - c_s)}{\Delta m_{43}^2} \quad (3.15)$$

we have for the solar sector

$$\epsilon_4 - \epsilon_3 = \Delta m_{43}^2 \left[\left| 1 - y'_e e^{2i\gamma'_e} - y'_s e^{2i\gamma'_s} \right|^2 - 4y'_e y'_s \sin 2\gamma'_e \sin 2\gamma'_s \sin^2 \frac{\delta'}{2} \right]^{1/2}. \quad (3.16)$$

Looking at Eq.(3.3) or Tab. I it can be read off that a_{CC} is not necessarily smaller than Δm_{21}^2 relevant for LBL neutrino oscillations and thus $\epsilon_2 - \epsilon_1$ could be different from Δm_{21}^2 . Since Δm_{43}^2 is of the order 10^{-5} or 10^{-10} eV², in the solar sector a_{CC} is much larger than the relevant mass-squared difference Δm_{sun}^2 except for reactor experiments with the MSW solution of the solar neutrino puzzle (see Tab. I). In any case, $\epsilon_4 - \epsilon_3 \simeq \Delta m^2$ holds and therefore the LBL oscillation probabilities averaged over the fast oscillations due to Δm^2 are given by

$$P_{\nu_\alpha \rightarrow \nu_\beta}^{(\text{LBL,A})} = \left| \sum_{j=1,2} U'_{\beta j} U'_{\alpha j} \exp\left(-i \frac{\epsilon_j}{2p} L\right) \right|^2 + \left| \sum_{k=3,4} U'_{\beta k} U'_{\alpha k} \exp\left(-i \frac{\epsilon_k}{2p} L\right) \right|^2, \quad (3.17)$$

analogously to the vacuum case (see Eqs.(2.1) and (2.2)).

A first upper bound on $P_{\nu_\alpha \rightarrow \nu_\beta}^{(\text{LBL})}$ is obtained by simply applying the Cauchy–Schwarz inequality to Eq.(3.17). Taking into account Eq.(3.10) this leads to

$$P_{\nu_\alpha \rightarrow \nu_\beta}^{(\text{LBL})} \leq c_\alpha c_\beta + (1 - c_\alpha)(1 - c_\beta). \quad (3.18)$$

It is remarkable that with Eq.(3.18) we have recovered Eq.(2.15) of the vacuum case. The present discussion reveals that this equation is correct in matter apart from terms of order $a_{CC}/\Delta m^2$. Eq.(3.18) is also valid for antineutrinos because the unitary matrix which

diagonalizes $H_{\bar{\nu}}$ also has the block structure (3.8) and in Eq.(3.10) the phases of U do not enter.

To derive matter corrections to the other bounds developed in section II it is convenient to write Eq.(3.17) in the form

$$P_{\nu_{\alpha} \rightarrow \nu_{\beta}}^{(\text{LBL,A})} = P'_{\nu_{\alpha} \rightarrow \nu_{\beta}} - 2 \text{Re} [U'_{\alpha 3} U'_{\beta 3} U'^*_{\alpha 4} U'_{\beta 4} (1 - \exp(-i\omega))] \quad (3.19)$$

where

$$P'_{\nu_{\alpha} \rightarrow \nu_{\beta}} = \left| U'_{\beta 1} U'^*_{\alpha 1} + U'_{\beta 2} U'^*_{\alpha 2} \exp\left(-i \frac{\epsilon_2 - \epsilon_1}{2p} L\right) \right|^2 + |U'_{\beta 3} U'^*_{\alpha 3} + U'_{\beta 4} U'^*_{\alpha 4}|^2 \quad (3.20)$$

and

$$\omega \equiv \frac{\epsilon_4 - \epsilon_3}{2p} L. \quad (3.21)$$

The Cauchy–Schwarz inequality and Eqs.(3.9) and (3.10) allow to bound the expression Eq.(3.20) for $\alpha \neq \beta$ by

$$\frac{1}{4} A_{\alpha;\beta} \leq P'_{\nu_{\alpha} \rightarrow \nu_{\beta}} \leq c_{\alpha} c_{\beta} + \frac{1}{4} A_{\alpha;\beta}. \quad (3.22)$$

For $\alpha = \beta$ we have instead

$$(1 - c_{\alpha})^2 \leq P'_{\nu_{\alpha} \rightarrow \nu_{\alpha}} \leq c_{\alpha}^2 + (1 - c_{\alpha})^2. \quad (3.23)$$

These two equations are the analogues of Eqs.(2.6) and (2.5), respectively. Matter corrections are characterized by the parameter ω . For $\omega = 0$ the vacuum bounds on $P_{\nu_{\alpha} \rightarrow \nu_{\beta}}^{(\text{LBL})}$ ensue. Inspection of Eq.(3.16) shows that, taking into account Eqs.(3.3) and (3.4), if $y'_{e,s} \gg 1$ the maximal value of the parameter ω is given by

$$\omega_{\max} \simeq \frac{3}{2} \frac{a_{CC} L}{2p} = \frac{3}{2} \sqrt{2} G_F N_e L = 8.6 \times 10^{-4} \left(\frac{L}{1\text{km}} \right) \quad (3.24)$$

for $\rho = 3 \text{ g cm}^{-3}$. Note that in this case ω_{\max} does not depend on the neutrino energy, but only on the propagation distance L . Hence, the matter corrections to the bounds for the LBL transition probabilities that we will derive in the case $y'_{e,s} \gg 1$ are independent from the neutrino energy and the corresponding bounds apply to all the energy spectrum of LBL experiments. From Eq.(3.24) one can see that these matter corrections could be relevant for $L \gtrsim 100 \text{ km}$. The size of ω_{\max} in the individual LBL experiments can be looked up in Tab. I. This parameter is not small for the MINOS and ICARUS experiments. In Tab. I the CHOOZ and Palo Verde experiments are not listed because their respective neutrino beams do not propagate in matter. Anyway, for baselines around 1 km matter effects are totally negligible, as can be seen from Eqs.(3.19)–(3.24).

The condition $y'_{e,s} \gg 1$ is satisfied in all the LBL experiments of the first generation if Δm_{sun}^2 is either in the range of the MSW or of the vacuum oscillation solution of the solar neutrino problem, apart from the LBL reactor experiments if the MSW effect is responsible for the solar neutrino deficit. In this case we have $\Delta m_{\text{sun}}^2 \gg a_{CC}$, which implies that $y'_{e,s} \ll 1$

and $\omega \simeq \eta$ given in Eq.(2.17). Furthermore, since in this case a_{CC} is much smaller than all the Δm^2 's, the mixing matrix in matter is the same as in vacuum and the oscillations in LBL reactor experiments are the same as in vacuum. Hence, this case coincides with that discussed in section II B.

For the same reasons as in the case of Eq.(3.18), the two inequalities (3.22) and (3.23) also hold for antineutrinos. The oscillation probabilities for scheme B follow from Eq.(3.17) with the substitution of indices

$$1, 2 \leftrightarrow 3, 4. \quad (3.25)$$

Since the conditions (1.12) for scheme B emerge from the corresponding conditions (1.11) through the same substitution (3.25), all the bounds derived for the scheme A hold likewise for the scheme B.

A. A bound on $P_{\nu_\mu \rightarrow \nu_e}^{(\text{LBL})}$ stable against matter effects

Repeating the discussion of section II for completeness, the bound (3.18) is non-trivial for the case of $\nu_\mu \rightarrow \nu_e$ transitions and thus we obtain

$$P_{\nu_\mu \rightarrow \nu_e}^{(\text{LBL})} \leq a_e^0 + a_\mu^0 - 2a_e^0 a_\mu^0. \quad (3.26)$$

As argued before it holds for both schemes A and B and for neutrinos and antineutrinos. In Figs. 2 and 3 the upper bound (3.26) is represented by the dotted curve.

B. The bound on $P_{\nu_e \rightarrow \nu_e}^{(\text{LBL})}$

From Eqs.(3.19) and (3.23) with $\alpha = \beta = e$ we get the lower bound

$$\begin{aligned} P_{\nu_e \rightarrow \nu_e}^{(\text{LBL,A})} &\geq (1 - c_e)^2 - 2|U'_{e3}|^2 |U'_{e4}|^2 (1 - \cos \omega) \\ &\geq (1 - c_e)^2 \cos^2 \frac{\omega}{2}. \end{aligned} \quad (3.27)$$

Finally, with Eq.(1.11) we arrive at the result

$$1 - P_{\nu_e \rightarrow \nu_e}^{(\text{LBL})} \leq 1 - \cos^2 \frac{\omega}{2} (1 - a_e^0)^2. \quad (3.28)$$

In the approximation $y'_{e,s} \gg 1$ the parameter ω is equal for neutrinos and antineutrinos. Therefore, like the bound (3.26), Eq.(3.28) holds for both schemes and for neutrinos and antineutrinos.

Taking into account the value of ω_{max} for the Kam-Land experiment in the case of a vacuum oscillation solution of the solar neutrino problem (see Tab. I), this equation shows that matter effects are not negligible in establishing the upper bound for $1 - P_{\bar{\nu}_e \rightarrow \bar{\nu}_e}^{(\text{LBL})}$ in this experiment. This upper bound is shown by the solid line in Fig. 4 and one can see that there is a small deviation from the vacuum bound (short-dashed line) for small values of Δm^2 . However, the vacuum bound is not substantially modified and the bound in matter is

well below the sensitivity of the Kam-Land experiment (represented by vertical long-dashed line). Hence, in the case of a vacuum oscillation solution of the solar neutrino problem the sensitivity of the Kam-Land experiment is not enough to observe $\bar{\nu}_e \rightarrow \bar{\nu}_e$ in the framework of the 4-neutrino schemes (1.3).

Conservation of probability leads to

$$P_{\nu_e \rightarrow \nu_\mu}^{(\text{LBL})} \leq 1 - P_{\nu_e \rightarrow \nu_e}^{(\text{LBL})} \quad (3.29)$$

and therefore Eq.(3.28) also bounds $P_{\nu_e \rightarrow \nu_\mu}^{(\text{LBL})}$. In LBL accelerator experiments, the initial neutrinos are ν_μ 's and not ν_e 's. If, however, CP is conserved in the lepton sector, it follows from the CPT theorem that the transition probabilities in vacuum are invariant under time reversal, i.e. $P_{\nu_\alpha \rightarrow \nu_\beta} = P_{\nu_\beta \rightarrow \nu_\alpha}$. In this case, the probabilities of $\nu_\alpha \rightarrow \nu_\beta$ and $\nu_\beta \rightarrow \nu_\alpha$ transitions are equal also in matter if the matter density is symmetric along the neutrino path. In general, however, these two probabilities are different. Nevertheless, from conservation of probability we obtain

$$P_{\nu_\mu \rightarrow \nu_e}^{(\text{LBL})} \leq 1 - P_{\nu_e \rightarrow \nu_e}^{(\text{LBL})} \leq 1 - \cos^2 \frac{\omega}{2} (1 - a_e^0)^2 . \quad (3.30)$$

Eq.(3.30) is the matter-corrected version of Eq.(2.12). For the K2K experiment $\sin^2 \omega_{\max} \simeq 10^{-2}$ is small, but for the ICARUS and MINOS experiments we obtain $\sin^2 \omega_{\max} \simeq 0.09$ and therefore, in the case of these two experiments, matter effects are considerable in the bound (3.30) on the probabilities of LBL $\nu_\mu \rightarrow \nu_e$ transitions. In Figs. 2 and 3 the long-dashed lines show the bound (3.30) for the K2K experiment and the ICARUS and MINOS experiments, respectively.

Note that the right-hand side of Eq.(3.28) also constitutes an upper bound for $P_{\nu_e \rightarrow \nu_\tau}^{(\text{LBL})}$.

C. The upper bound on $P_{\nu_\mu \rightarrow \nu_e}^{(\text{LBL})}$

Now we come to matter corrections to the bound (2.9) on $P_{\nu_\mu \rightarrow \nu_e}^{(\text{LBL})}$ which incorporates information on $A_{\mu;e}$. The starting point is given by Eqs.(3.19) and (3.22). To proceed further it is necessary to develop a parameterization for $U'_{\alpha j}$. Without loss of generality we can write

$$U'_{ej} = \sqrt{1 - c_e} e_{j-2}^{(1)} \quad \text{for} \quad j = 3, 4, \quad (3.31)$$

with the orthonormal basis

$$e^{(1)}(\theta) = (\cos \theta, \sin \theta), \quad e^{(2)}(\theta) = (-\sin \theta, \cos \theta). \quad (3.32)$$

We expand $U'_{\mu j}$ with $j = 3, 4$ with respect to this basis as

$$U'_{\mu j} = \sqrt{1 - c_\mu} \sum_{\rho=1,2} p_\rho e_{j-2}^{(\rho)}, \quad (3.33)$$

where p_1 and p_2 are complex coefficients such that

$$\sum_{\rho=1,2} |p_\rho|^2 = 1. \quad (3.34)$$

Using this parameterization, from Eqs.(1.6) and (3.9) we obtain

$$A_{\mu;e} = 4(1 - c_e)(1 - c_\mu)|p_1|^2. \quad (3.35)$$

With these equations we eliminate $|p_1|$ and $|p_2|$ and defining $\sigma = \arg(p_1^* p_2)$ we arrive at

$$\begin{aligned} P_{\nu_\mu \rightarrow \nu_e}^{(\text{LBL})} &\leq c_e c_\mu + \frac{1}{4} A_{\mu;e} + (1 - \cos \omega) \left\{ \left[\frac{1}{2} (1 - c_e)(1 - c_\mu) - \frac{1}{4} A_{\mu;e} \right] \sin^2 2\theta - \right. \\ &\quad \left. - \frac{1}{8} \sqrt{A_{\mu;e} [4(1 - c_e)(1 - c_\mu) - A_{\mu;e}]} \sin 4\theta \cos \sigma \right\} - \\ &\quad - \frac{1}{4} \sin \omega \sqrt{A_{\mu;e} [4(1 - c_e)(1 - c_\mu) - A_{\mu;e}]} \sin 2\theta \sin \sigma. \end{aligned} \quad (3.36)$$

Since we do not have information on the values of θ and σ , we have to maximize the right-hand side of Eq.(3.36). The maximum with respect to σ is easily found: the maximum of a function $a \cos \sigma + b \sin \sigma$ with constant a and b is given by $\sqrt{a^2 + b^2}$. It remains to find the maximum with respect to $\sin^2 2\theta$ for the resulting function. One can show that, if $\cos \omega \geq 0$, the maximum is given by $\sin^2 2\theta = 1$. This is the case for the K2K, MINOS and ICARUS experiments because $\omega_{\text{max}} < \pi/2$ and therefore the following bound applies:

$$\begin{aligned} P_{\nu_\mu \rightarrow \nu_e}^{(\text{LBL})} &\leq c_e c_\mu + \frac{1}{4} \cos \omega A_{\mu;e} + \frac{1}{2} (1 - \cos \omega) (1 - c_e) (1 - c_\mu) + \\ &\quad + \frac{1}{4} \sin \omega \sqrt{A_{\mu;e} [4(1 - c_e)(1 - c_\mu) - A_{\mu;e}]}. \end{aligned} \quad (3.37)$$

In this inequality it is difficult to take into account analytically the conditions (1.11), (1.15) and $\omega \leq \omega_{\text{max}}$. Hence, we have done it numerically and the result is shown by the solid curves in Figs. 2 and 3. In both figures the solid curve is the most stringent bound on $\bar{\nu}_\mu \rightarrow \bar{\nu}_e$ transitions with matter effects. These two solid curves belong to the main results of this paper. It is interesting to compare the solid curves in Figs. 2 and 3 with the short-dashed lines which represent the corresponding bounds in vacuum. For the K2K experiment the solid line deviates from the short-dashed line only at Δm^2 close to 0.3 eV^2 , the lower edge of the range (1.2). The same is true for the MINOS and ICARUS experiments except that the deviation starts at larger Δm^2 values and is more pronounced at the lower edge of the shadowed area.

As in the previous sections, the bound (3.37) is valid for neutrinos and antineutrinos. Although the parameters θ and σ are in principle different for neutrinos and antineutrinos the maximization procedure wipes out any difference in the bounds.

D. The lower bound on $P_{\nu_\mu \rightarrow \nu_e}^{(\text{LBL})}$

Since the LSND experiment has seen a positive signal for $P_{\bar{\nu}_\mu \rightarrow \bar{\nu}_e}^{(\text{LBL})}$, this experiment provides a lower bound for the amplitude of $\bar{\nu}_\mu \rightarrow \bar{\nu}_e$ transitions (see Eq.(2.14)). Using analogous steps as in the previous section one derives

$$P_{\nu_\mu \rightarrow \nu_e}^{(\text{LBL})} \geq \frac{1}{4} \cos \omega A_{\mu;e} + \frac{1}{2} (1 - \cos \omega) (1 - c_e) (1 - c_\mu) - \frac{1}{4} \sin \omega \sqrt{A_{\mu;e} [4(1 - c_e)(1 - c_\mu) - A_{\mu;e}]}. \quad (3.38)$$

Now we have to minimize the right-hand side of Eq.(3.38) with respect to c_e and c_μ with the bounds (1.11). This procedure leads to the following result:

$$P_{\nu_\mu \rightarrow \nu_e}^{(\text{LBL})} \geq 0 \quad \text{for} \quad A_{\mu;e} \leq 2(1 - \cos \omega) a_\mu^0 \quad (3.39)$$

and

$$P_{\nu_\mu \rightarrow \nu_e}^{(\text{LBL})} \geq \frac{1}{4} \cos \omega A_{\mu;e} + \frac{1}{2} (1 - \cos \omega) a_\mu^0 - \frac{1}{4} \sin \omega \sqrt{A_{\mu;e} (4a_\mu^0 - A_{\mu;e})} \quad (3.40)$$

for $A_{\mu;e} \geq 2(1 - \cos \omega) a_\mu^0$.

Eq.(3.39) states that $A_{\mu;e}$ has to be sufficiently large otherwise the non-trivial lower bound in vacuum ($\omega = 0$) becomes trivial.

Taking $\omega = 0.63$, the maximal value of the parameter ω for the ICARUS and MINOS experiments (see Tab. I), the condition for a trivial lower bound on $P_{\nu_\mu \rightarrow \nu_e}^{(\text{LBL})}$ is given by $A_{\mu;e} \lesssim 0.3 a_\mu^0$. Looking at $A_{\mu;e}^{\text{min}}$ of the LSND experiment and the function a_μ^0 one sees that indeed this condition is fulfilled. Thus matter effects make the non-trivial lower bound of the vacuum case disappear. For the K2K experiment the analogous condition for triviality is given by $A_{\mu;e} \lesssim 0.04 a_\mu^0$. Here the triviality condition is not fulfilled but K2K does not seem to have sufficient sensitivity to reach small enough $P_{\nu_\mu \rightarrow \nu_e}^{(\text{LBL})}$. However, for such small oscillation probabilities it would be necessary to take corrections of order $a_{CC}/\Delta m^2$ into account. Thus also in this case the lower bound seems to be irrelevant and the shadowed areas (dark and light) in Figs. 2 and 3 show the allowed regions for $\nu_\mu \rightarrow \nu_e$ transitions taking into account matter effects for the K2K experiment (Fig. 2) and the MINOS and ICARUS experiments (Fig. 3).

IV. THREE MASSIVE NEUTRINOS

It is worthwhile to have a look at LBL neutrino oscillation experiments neglecting some of the present hints for neutrino oscillations. It is possible that not all these hints will be substantiated in the course of time and it is useful to check which features are actually dependent on or independent from them.

In this section we consider the minimal scenario of mixing of three neutrinos. We will assume that of the two differences of squares of neutrino masses one is relevant for SBL oscillations and the other one for LBL oscillations (see also Refs. [40–42]). Hence, in this section we adopt the point of view that not neutrino mixing but other reasons could explain the solar neutrino data. With these assumptions, there are two possible 3-neutrino mass spectra:

$$(I) \quad \underbrace{m_1 < m_2 \ll m_3}_{\text{SBL}} \quad \text{LBL} \quad \text{and} \quad (II) \quad \underbrace{m_1 \ll m_2 < m_3}_{\text{SBL}} \quad \text{LBL}. \quad (4.1)$$

In both schemes I and II, Δm_{31}^2 is assumed to be relevant for neutrino oscillations in SBL experiments. In this case, the SBL oscillation probabilities depend on $|U_{e3}|^2$ and $|U_{\mu 3}|^2$ in the scheme I [37] and on $|U_{e1}|^2$ and $|U_{\mu 1}|^2$ in the scheme II [28]. There are three regions of these quantities which are allowed by the results of disappearance experiments (see Refs. [37,28]):

$$\begin{aligned}
(1) \quad & |U_{ek}|^2 \geq 1 - a_e^0, & |U_{\mu k}|^2 \leq a_\mu^0, \\
(2) \quad & |U_{ek}|^2 \leq a_e^0, & |U_{\mu k}|^2 \leq a_\mu^0, \\
(3) \quad & |U_{ek}|^2 \leq a_e^0, & |U_{\mu k}|^2 \geq 1 - a_\mu^0,
\end{aligned} \tag{4.2}$$

with $k = 3$ for the scheme I and $k = 1$ for the scheme II² (for the definition of a_e^0 and a_μ^0 see Eq.(1.14)).

The neutrino and antineutrino LBL oscillation probabilities in scheme I are given by

$$P_{\nu_\alpha \rightarrow \nu_\beta}^{(\text{LBL}, \text{I})} = \left| U_{\beta 1} U_{\alpha 1}^* + U_{\beta 2} U_{\alpha 2}^* \exp\left(-i \frac{\Delta m_{21}^2 L}{2p}\right) \right|^2 + |U_{\beta 3}|^2 |U_{\alpha 3}|^2, \tag{4.3}$$

$$P_{\bar{\nu}_\alpha \rightarrow \bar{\nu}_\beta}^{(\text{LBL}, \text{I})} = \left| U_{\beta 1}^* U_{\alpha 1} + U_{\beta 2}^* U_{\alpha 2} \exp\left(-i \frac{\Delta m_{21}^2 L}{2p}\right) \right|^2 + |U_{\beta 3}|^2 |U_{\alpha 3}|^2. \tag{4.4}$$

The transition probabilities in the scheme II can be obtained from the expressions (4.3) and (4.4) with the cyclic permutation of the indices

$$1, 2, 3 \rightarrow 2, 3, 1. \tag{4.5}$$

Therefore, as in the case of the schemes A and B for four neutrinos, the bounds on the LBL oscillation probabilities are the same in the 3-neutrino schemes I and II. In the following we will concentrate on scheme I.

The bounds on the vacuum LBL oscillation probabilities $P_{\nu_\alpha \rightarrow \nu_\beta}^{(\text{LBL})}$ for the 4-neutrino schemes (1.3) are valid also in the case of mixing of three neutrinos: the demonstrations in the 4-neutrino case A (B) can be carried over to the 3-neutrino case I (II) if we put $U_{\alpha 4} = 0$ ($U_{\alpha 1} = 0$ and change the indices $2, 3, 4 \rightarrow 1, 2, 3$) for all $\alpha = e, \mu, \tau$. It is obvious that, with $A_{\alpha; \beta} = 4|U_{\beta 3}|^2 |U_{\alpha 3}|^2$, the same bounds on $P_{\nu_\alpha \rightarrow \nu_\beta}^{(\text{LBL})}$ arise for $\alpha = \beta$ and $\alpha \neq \beta$ as given by Eqs.(2.5) and (2.6).

It is interesting to observe that in the 3-neutrino case there are no matter corrections, apart from those of order $a_{CC}/\Delta m^2$ which have been neglected also in the 4-neutrino case. This is easily understood by noting that the matrix R (3.8) has now a 1×1 block R_{sun} . Consequently, there is no analogue to the eigenvalue ϵ_4 of R . This situation corresponds to $\omega = 0$ and vanishing matter corrections at the order we are interested in. Let us emphasize

² For a comparison, the schemes I, II and the regions 1, 2, 3 are called hierarchies II, I and regions A, B, C, respectively, in Ref. [40].

that this absence of matter corrections is relative to the bounds on the oscillation probabilities which we are discussing, but in general the oscillation probabilities are affected by matter effects through R_{atm} and $\epsilon_2 - \epsilon_1$.

In the following we will give the bounds on the LBL oscillation probabilities for each of the regions (4.2), along the lines of the 4-neutrino section II.

Region 1. With respect to SBL and LBL neutrino oscillations, the 3-neutrino schemes I and II in region 1 correspond to the 4-neutrino schemes A and B, respectively, with the same bounds on $P_{\nu_e \rightarrow \nu_e}^{(\text{LBL})}$ (Eq.(2.7) and Fig. 1) and $P_{\nu_\mu \rightarrow \nu_e}^{(\text{LBL})}$ (Eqs.(2.13) and (2.16) and Figs. 2 and 3).

For completeness, we want to mention that there is a change in the upper bound for $P_{\nu_\mu \rightarrow \nu_e}^{(\text{LBL})}$ in going from four to three neutrinos: taking into account the inequality $c_e + c_\mu \geq 1$, we have $c_\mu \geq 1 - \min(a_e^0, a_\mu^0)$ and Eq.(2.16) improves to

$$P_{\nu_\mu \rightarrow \nu_e}^{(\text{LBL})} \leq a_e^0 + (1 - 2a_e^0) \min(a_e^0, a_\mu^0) . \quad (4.6)$$

For $a_e^0 < a_\mu^0$ this bound is slightly more stringent than that given by Eq.(2.12), but the improvement is negligible for $a_e^0 \ll 1$.

Region 2. Actually, this region is excluded by the results of the LSND experiment (see Refs. [37,28,29]) apart from a small interval of Δm^2 which might be marginally allowed. The reason is that (in combination with other data) the upper bound

$$A_{\mu:e} \leq 4 a_e^0 a_\mu^0 \quad (4.7)$$

is too restrictive to be compatible with the LSND data. In spite of this evidence, let us discuss the bounds on the LBL probabilities in this region.

The restrictions $c_e \geq 1 - a_e^0$, $c_\mu \geq 1 - a_\mu^0$ and the unitarity of the mixing matrix imply that c_τ is small: $c_\tau = 2 - c_e - c_\mu \leq a_e^0 + a_\mu^0$. From Eq.(2.6) it follows that the probabilities of $\nu_\mu \rightarrow \nu_\tau$ and $\nu_e \rightarrow \nu_\tau$ transitions in LBL experiments are confined in the range

$$\frac{1}{4} A_{\alpha;\tau} \leq P_{\nu_\alpha \rightarrow \nu_\tau}^{(\text{LBL})} \leq \frac{1}{4} A_{\alpha;\tau} + a_e^0 + a_\mu^0 \quad (\alpha = e, \mu) , \quad (4.8)$$

whereas for the probability of $\nu_\mu \rightarrow \nu_e$ transitions we have only the lower bound

$$\frac{1}{4} A_{\mu:e} \leq P_{\nu_\mu \rightarrow \nu_e}^{(\text{LBL})} . \quad (4.9)$$

The inequality (2.11) leads to the additional upper bounds

$$P_{\nu_\alpha \rightarrow \nu_\tau}^{(\text{LBL})} \leq (a_e^0 + a_\mu^0) (2 - a_e^0 - a_\mu^0) \quad (\alpha = e, \mu) . \quad (4.10)$$

We want to mention that the scenario of Ref. [31] is settled in region 2 and seems to take advantage of the fact that $\Delta m^2 \simeq 1.7 \text{ eV}^2$ is marginally allowed despite of Eq.(4.7) (see Refs. [29,34]). In this way Ref. [31] incorporates the LSND data whereas the atmospheric neutrino anomaly and the solar neutrino deficit are taken into account by a single $\Delta m_{\text{atm,sun}}^2 \sim$

10^{-2} eV^2 , which allows for the zenith angle variation of the atmospheric neutrino anomaly but leads to an energy-independent suppression of the solar neutrino flux that is unfavoured by the data of solar neutrino experiments [43,44]. Moreover, it has been shown in Ref. [33] that a combined analysis of all SBL data excludes this scenario at $\sim 99\%$ CL.

Region 3. In this region, where $c_e \geq 1 - a_e^0$ and $c_\mu \leq a_\mu^0$, the full set of atmospheric neutrino data cannot be explained in the framework discussed here. The reason is that for sub-GeV events one has

$$P_{\nu_\mu \rightarrow \nu_\mu}^{(\text{LBL})} \geq (1 - a_\mu^0)^2 \quad (4.11)$$

and this is incompatible [29] with the atmospheric neutrino anomaly except for values of Δm^2 close to 0.3 eV^2 , where there is no zenith-angle variation. The LBL transition probabilities of muon neutrinos are confined by

$$\frac{1}{4} A_{\mu;\beta} \leq P_{\nu_\mu \rightarrow \nu_\beta}^{(\text{LBL})} \leq \frac{1}{4} A_{\mu;\beta} + a_\mu^0 \quad (\beta = e, \tau), \quad (4.12)$$

whereas for $\nu_e \rightarrow \nu_\tau$ transitions there is only the lower bound

$$\frac{1}{4} A_{e;\tau} \leq P_{\nu_e \rightarrow \nu_\tau}^{(\text{LBL})}. \quad (4.13)$$

The inequality (2.10), which is a consequence of probability conservation, leads to

$$P_{\nu_\mu \rightarrow \nu_\beta}^{(\text{LBL})} \leq a_\mu^0 (2 - a_\mu^0) \quad (\beta = e, \tau). \quad (4.14)$$

Furthermore, taking into account the inequality $c_e + c_\mu \geq 1$, we have $c_e \geq 1 - \min(a_e^0, a_\mu^0)$ and Eq.(2.16) improves to

$$P_{\nu_\mu \rightarrow \nu_e}^{(\text{LBL})} \leq a_\mu^0 + (1 - 2a_\mu^0) \min(a_e^0, a_\mu^0). \quad (4.15)$$

For $a_e^0 \ll a_\mu^0 \ll 1$ this bound is about half of that given by Eq.(4.14).

The 3-neutrino scheme of Ref. [32], which lies in region 3, merges the LSND and atmospheric mass-squared scales and dispenses with the zenith angle variation of the atmospheric neutrino anomaly. This is only allowed at $\Delta m^2 \simeq 0.3 \text{ eV}^2$ (see also Ref. [33]). If one accepts this possibility, the low mass-squared difference is free to be used for a solution of the solar neutrino deficit problem.

The differences in the bounds on the LBL probabilities are marked and could thus serve to distinguish between the three different regions in the 3-neutrino case. They also serve as a cross-check for present hints of neutrino oscillations. Of course, in the experiments discussed the bounds on the transition probabilities in vacuum in the 4-neutrino case (schemes A and B) are indistinguishable from those in the 3-neutrino case with region 1. However, LBL experiments could distinguish the 4-neutrino case from the 3-neutrino case by measuring a transition probability $P_{\nu_\mu \rightarrow \nu_e}^{(\text{SBL})}$ or a survival probability $P_{\bar{\nu}_e \rightarrow \bar{\nu}_e}^{(\text{LBL})}$ which is incompatible with the vacuum bounds but satisfies the bounds in matter obtained in the 4-neutrino case. Such an observation would exclude the 3-neutrino case with region 1.

V. CONCLUSIONS

At present there are three experimental indications in favour of neutrino oscillations which correspond to three different scales of neutrino mass-squared differences: the solar neutrino deficit, the atmospheric neutrino anomaly and the result of the LSND experiment. These indications and the negative results of numerous short-baseline neutrino experiments can be accommodated in two schemes (A and B) with mixing of four massive neutrinos [29]. In this paper we have presented a detailed study of the predictions of the schemes A and B for long-baseline experiments. We have discussed what general conclusions on the long-baseline transition probabilities between different neutrino states can be inferred from the existing data of short-baseline experiments, taking into account the results of solar and atmospheric neutrino experiments. We have obtained rather strong bounds on the probabilities of $\bar{\nu}_e \rightarrow \bar{\nu}_e$ and $\bar{\nu}_\mu \rightarrow \bar{\nu}_e$ LBL transitions. Matter effects were thoroughly taken into account and we have shown that they do not change substantially the main conclusions drawn from the vacuum case.

The schemes A and B give completely different predictions for neutrinoless double beta decay and for neutrino mass effects in experiments for neutrino mass measurements by the tritium method [29]. They lead, however, to the same bounds on long-baseline oscillation probabilities. In addition, all the bounds that we have derived apply for neutrinos as well as antineutrinos.

We have shown that the results of the short-baseline reactor experiments put rather severe bounds on the probability $1 - P_{\bar{\nu}_e \rightarrow \bar{\nu}_e}^{(\text{LBL})}$ of $\bar{\nu}_e$ transitions into all possible other states in the long-baseline CHOOZ and Palo Verde reactor experiments. If the Δm^2 relevant in short-baseline oscillations is bigger than about 3 eV^2 , the bound on $1 - P_{\bar{\nu}_e \rightarrow \bar{\nu}_e}^{(\text{LBL})}$ is slightly higher than the sensitivity of the CHOOZ experiment, allowing some possibility to reveal neutrino oscillations in this channel. However, the results of the LSND experiment favour the range $0.3 \lesssim \Delta m^2 \lesssim 2.2 \text{ eV}^2$. We have shown that in this range the upper bound for the quantity $1 - P_{\bar{\nu}_e \rightarrow \bar{\nu}_e}^{(\text{LBL})}$ lies between 10^{-2} and 5×10^{-2} (see Fig. 1) and thus is below the sensitivity of CHOOZ and Palo Verde.

The Kam-Land reactor experiment is very interesting because its baseline of 150 km is very long compared to the baseline of 1 km of CHOOZ and Palo Verde. If the solar neutrino deficit problem is to be resolved by vacuum oscillations, the situation is very similar to the other LBL reactor experiments. The upper bound on $1 - P_{\bar{\nu}_e \rightarrow \bar{\nu}_e}^{(\text{LBL})}$ is shown in Fig. 4 by the solid line. It deviates from the short-dashed curve, which is valid in vacuum, because matter corrections are not negligible though small in this case, due to the long baseline. The bound represented by the short-dashed curve in Fig. 4 is valid also in the case of a small mixing angle MSW solution of the solar neutrino problem. On the other hand, we have shown in section II B that, if large mixing angle MSW resonant flavour transitions are responsible for the solar neutrino deficit, the bound on $1 - P_{\bar{\nu}_e \rightarrow \bar{\nu}_e}^{(\text{LBL})}$ in Kam-Land becomes practically trivial at small neutrino energies ($\sim 1 \text{ MeV}$). Therefore, if in the Kam-Land experiment a large value of $1 - P_{\bar{\nu}_e \rightarrow \bar{\nu}_e}^{(\text{LBL})}$ is found at small neutrino energies, with a suppression at higher neutrino energies, we would have an indirect indication in favour of the large mixing angle MSW solution of the solar neutrino deficit.

We have also shown that in this case Δm_{sun}^2 could be determined by measuring the

maxima of $P_{\bar{\nu}_e \rightarrow \bar{\nu}_e}^{(\text{LBL})}$ as a function of the neutrino energy. There are two conditions that must be satisfied in a LBL experiment in order to have the possibility to measure Δm_{sun}^2 , apart from the necessary sensitivity and energy resolution. First one needs $\Delta m_{\text{sun}}^2 \gg a_{CC}$ in order that this measurement is not disturbed by matter effects. Second, $\Delta m_{\text{sun}}^2 L/2p \sim 1$ is required. These conditions lead to $p \ll 40$ MeV and $L \sim 40 \times (p/1 \text{ MeV})$ km for $\Delta m_{\text{sun}}^2 \sim 10^{-5}$ eV². At present, among the planned LBL experiments these conditions are only met by Kam-Land.

In Figs. 2 and 3 the solid lines depict the upper bounds on the probability $P_{\nu_{\mu} \rightarrow \nu_e}^{(\text{LBL})}$ of $\nu_{\mu} \rightarrow \nu_e$ transitions for the K2K experiment and the MINOS and ICARUS experiments, respectively. In the derivation of the solid curves matter effects are included and thus in the schemes A and B such transitions are severely constrained by the results of short-baseline reactor and accelerator experiments. The sensitivities of MINOS and ICARUS is well below the upper bound for $P_{\nu_{\mu} \rightarrow \nu_e}^{(\text{LBL})}$ whereas the sensitivity of the K2K experiment might be insufficient. If matter effects are neglected, the upper bound on this probability is given by the short-dashed lines in Figs. 2 and 3. In all four figures the shadowed regions (light and dark) indicate the range (1.2) determined by the LSND experiment and the negative results of all the other SBL experiments.

We have shown that there is also an upper bound on long-baseline $\nu_e \rightarrow \nu_{\tau}$ oscillations which is less tight than the one for $\nu_{\mu} \rightarrow \nu_e$ transitions. It is indicated by the long-dashed curves in Figs. 2 and 3 which would be relevant if the corresponding experiments would use a ν_e beam. On the other hand, the long-baseline $\nu_{\mu} \rightarrow \nu_{\mu}$ and $\nu_{\mu} \rightarrow \nu_{\tau}$ channels are unconstrained with the methods discussed here.

We have obtained bounds on LBL transition probabilities in the case of the neutrino mass spectra (1.3), which are implied by the results of the solar, atmospheric and LSND experiments. If the LSND data are not confirmed by future experiments, but nevertheless there is a mass (or masses) approximately equal to 1 eV providing an explanation for the hot dark matter problem, then the neutrino mass spectrum can be different from the spectra A and B in Eq.(1.3). The natural neutrino mass spectrum in this case is hierarchical and the bounds that we have obtained in this paper are not valid.

We have also made a digression to 3-neutrino scenarios and discussed the bounds on the transition probabilities for all possible cases such that the two mass-squared differences correspond to SBL and LBL neutrino oscillations. We have argued that for three neutrinos matter corrections to the bounds on the transition probabilities are absent, apart from those of order $a_{CC}/\Delta m^2$ which have been neglected also in the 4-neutrino case.

Summarizing, we would like to emphasize that the results of all neutrino oscillation experiments lead to severe constraints for the probabilities of $\bar{\nu}_e$ disappearance and $\nu_{\mu} \rightarrow \nu_e$ appearance in long-baseline experiments. Nevertheless, the allowed region for the probability in the $\nu_{\mu} \rightarrow \nu_e$ channel is well within the planned sensitivities of the MINOS and ICARUS experiments. The channels $\nu_{\mu} \rightarrow \nu_{\tau}$ and $\nu_{\mu} \rightarrow \nu_{\mu}$ are not constrained at all. Therefore, from the point of view of the present investigation, long-baseline muon neutrino beams provide promising facilities for the observation of neutrino oscillations. However, it is important to note that future measurements by LBL experiments of $\bar{\nu}_e \rightarrow \bar{\nu}_e$ and/or $\nu_{\mu} \rightarrow \nu_e$ transition

probabilities that violate the bounds presented in this paper would allow to exclude the 4-neutrino schemes (1.3).

NOTE ADDED

After we finished this paper the results of the first long-baseline reactor experiment CHOOZ appeared (M. Apollonio *et al.*, preprint hep-ex/9711002). No indications in favor of $\bar{\nu}_e \rightarrow \bar{\nu}_e$ transitions were found in this experiment. The upper bound for the transition probability of electron antineutrinos into other states found in the CHOOZ experiment is in agreement with the limit presented in Fig.1.

ACKNOWLEDGMENTS

C.G. would like to thank K. Inoue, E. Lisi, F. Martelli, H. Nunokawa, O. Peres, A. Rossi, V. Semikoz and F. Vetrano for useful discussions at TAUP97. S.M.B. like to acknowledge support from Dyson Visiting Professor Funds at the Institute for Advanced Study.

REFERENCES

- [1] S.M. Bilenky and B. Pontecorvo, Phys. Rep. **41**, 225 (1978).
- [2] S.M. Bilenky and S.T. Petcov, Rev. Mod. Phys. **59**, 671 (1987).
- [3] R.N. Mohapatra and P.B. Pal, *Massive Neutrinos in Physics and Astrophysics*, World Scientific Lecture Notes in Physics, Vol. 41 (Singapore, 1991).
- [4] C.W. Kim and A. Pevsner, *Neutrinos in Physics and Astrophysics*, Contemporary Concepts in Physics, Vol. 8, (Harwood Academic Press, Chur, Switzerland, 1993).
- [5] R.I. Steinberg, Proc. of the 5th *International Workshop on Neutrino Telescopes*, Venezia, March 1993.
- [6] F. Boehm *et al.*, *The Palo Verde experiment*, 1996 (<http://www.cco.caltech.edu/~songhoon/Palo-Verde/Palo-Verde.html>).
- [7] M. Nakahata, Talk presented at the *International Europhysics Conference on High Energy Physics*, 19-26 August 1997, Jerusalem, Israel (<http://www.cern.ch/hep97/abstract/tpl.htm>).
- [8] Y. Suzuki, Proc. of *Neutrino 96*, Helsinki, June 1996, edited by K. Enqvist *et. al.*, p. 237 (World Scientific, Singapore, 1997).
- [9] MINOS Coll., D. Ayres *et al.*, NUMI-L-63, February 1995.
- [10] ICARUS Coll., P. Cennini *et al.*, LNGS-94/99-I, May 1994.
- [11] B.T. Cleveland *et al.*, Nucl. Phys. B (Proc. Suppl.) **38**, 47 (1995).
- [12] K.S. Hirata *et al.*, Phys. Rev. D **44**, 2241 (1991).
- [13] GALLEX Coll., W. Hampel *et al.*, Phys. Lett. B **388**, 384 (1996).
- [14] J.N. Abdurashitov *et al.*, Phys. Rev. Lett. **77**, 4708 (1996).
- [15] K. Inoue, Talk presented at *TAUP97*, September 7-11, 1997, Laboratori Nazionali del Gran Sasso, Assergi (Italy).
- [16] Y. Fukuda *et al.*, Phys. Lett. B **335**, 237 (1994).
- [17] R. Becker-Szendy *et al.*, Nucl. Phys. B (Proc. Suppl.) **38**, 331 (1995).
- [18] W.W.M. Allison *et al.*, Phys. Lett. B **391**, 491 (1997).
- [19] K. Martens, Talk presented at the *International Europhysics Conference on High Energy Physics*, 19-26 August 1997, Jerusalem, Israel (<http://www.cern.ch/hep97/abstract/tpa10.htm>).
- [20] C. Athanassopoulos *et al.*, Phys. Rev. Lett. **77**, 3082 (1996).
- [21] V. Barger, R.J.N. Phillips and K. Whisnant, Phys. Rev. Lett. **69**, 3135 (1992); P.I. Krastev and S.T. Petcov, Phys. Rev. Lett. **72**, 1960 (1994).
- [22] S.P. Mikheyev and A.Yu. Smirnov, Yad. Fiz. **42**, 1441 (1985) [*Sov. J. Nucl. Phys.* **42**, 913 (1985)]; *Il Nuovo Cimento C* **9**, 17 (1986); L. Wolfenstein, Phys. Rev. D **17**, 2369 (1978); *ibid.* **20**, 2634 (1979).
- [23] GALLEX Coll., P. Anselmann *et al.*, Phys. Lett. B **285**, 390 (1992); P.I. Krastev and S.T. Petcov, *ibid.* **299**, 99 (1993); N. Hata and P.G. Langacker, Phys. Rev. D **50**, 632 (1994); G. Fiorentini *et al.*, *ibid.* **49**, 6298 (1994).
- [24] B. Achkar *et al.*, Nucl. Phys. B **434**, 503 (1995).
- [25] L. Borodovsky *et al.*, Phys. Rev. Lett. **68**, 274 (1992).
- [26] F. Boehm, Nucl. Phys. B (Proc. Suppl.) **48**, 148 (1996); F. Vannucci, *ibid.*, 154 (1996).
- [27] J.T. Peltoniemi and J.W.F. Valle, Nucl. Phys. B **406**, 409 (1993); D.O. Caldwell and R.N. Mohapatra, Phys. Rev. D **48**, 3259 (1993); Z. Berezhiani and R.N. Mohapatra,

- Phys. Rev. D **52**, 6607 (1995); J.R. Primack *et al.*, Phys. Rev. Lett. **74**, 2160 (1995); E. Ma and P. Roy, Phys. Rev. D **52**, R4780 (1995); R. Foot and R.R. Volkas, Phys. Rev. D **52**, 6595 (1995); E.J. Chun *et al.*, Phys. Lett. B **357**, 608 (1995); J.J. Gomez-Cadenas and M.C. Gonzalez-Garcia, Z. Phys. C **71**, 443 (1996); S. Goswami, Phys. Rev. D **55**, 2931 (1997); A.Yu. Smirnov and M. Tanimoto, Phys. Rev. D **55**, 1665 (1997); E. Ma, Mod. Phys. Lett. A **11**, 1893 (1996).
- [28] S.M. Bilenky *et al.*, Phys. Rev. D **54**, 4432 (1996).
- [29] S.M. Bilenky, C. Giunti and W. Grimus, preprint UWThPh-1996-42 (hep-ph/9607372), to appear in Z. Phys. C.
- [30] N. Okada and O. Yasuda, Int. J. Mod. Phys. A **12**, 3669 (1997).
- [31] A. Acker and S. Pakvasa, Phys. Lett. B **357**, 209 (1997).
- [32] C.Y. Cardall and G.M. Fuller, Phys. Rev. D **53**, 4421 (1996); C.Y. Cardall, G.M. Fuller and D.B. Cline, preprint hep-ph/9706426; E. Ma and P. Roy, preprint hep-ph/9706309.
- [33] G.L. Fogli *et al.*, Phys. Rev. D **56**, 4365 (1997).
- [34] S.M. Bilenky, C. Giunti and W. Grimus, preprint UWThPh-1997-17 (hep-ph/9707372).
- [35] F. Dydak *et al.*, Phys. Lett. B **134**, 281 (1984).
- [36] I.E. Stockdale *et al.*, Phys. Rev. Lett. **52**, 1384 (1984).
- [37] S.M. Bilenky *et al.*, Phys. Lett. B **356**, 273 (1995); Phys. Rev. D **54**, 1881 (1996).
- [38] L.A. Ahrens *et al.*, Phys. Rev. D **36**, 702 (1987).
- [39] A. Romosan *et al.*, Phys. Rev. Lett. **78**, 2912 (1997).
- [40] M. Tanimoto, Phys. Rev. D **55**, 322 (1997).
- [41] J. Arafune and J. Sato, Phys. Rev. D **55**, 1653 (1997); J. Arafune, M. Koike and J. Sato, Phys. Rev. D **56**, 3093 (1997).
- [42] H. Minakata and H. Nunokawa, preprint TMUP-HEL-9704 (hep-ph/9705208).
- [43] P.I. Krastev and S.T. Petcov, Phys. Rev. D **53**, 1665 (1996).
- [44] G. Conforto *et al.*, preprint UB/FI 97-1 (hep-ph/9708301).

TABLES

Experiment	$\langle p \rangle / 1 \text{ GeV}$	$L / 1 \text{ km}$	$a_{CC} / 1 \text{ eV}^2$	ω_{\max}
Kam-Land (vac. osc.)	10^{-3}	150	2.3×10^{-7}	0.13
K2K	1	250	2.3×10^{-4}	0.22
MINOS	10	730	2.3×10^{-3}	0.63
ICARUS	25	730	5.8×10^{-3}	0.63

TABLE I. List of the planned LBL experiments (except CHOOZ and Palo Verde where matter effects are absent) with their average neutrino momenta $\langle p \rangle$, the length L of the baseline, the value of the matter parameter a_{CC} and the maximal value of the phase ω (given by Eq.(3.24)) characterizing the matter effects in the bounds on LBL neutrino oscillation probabilities.

FIGURES

FIG.1. Upper bound for the transition probability $1 - P_{\bar{\nu}_e \rightarrow \bar{\nu}_e}^{(\text{LBL})}$ in the CHOOZ and Palo Verde experiments (solid curve), for Δm^2 in the range $10^{-1} \text{ eV}^2 \leq \Delta m^2 \leq 10^3 \text{ eV}^2$. The upper bound was obtained from the 90% CL exclusion plot of the Bugey $\bar{\nu}_e \rightarrow \bar{\nu}_e$ experiment [24]. The dash-dotted and dash-dot-dotted vertical lines depict, respectively, the expected sensitivities of the CHOOZ and Palo Verde LBL reactor neutrino experiments. The shaded region corresponds to the range of Δm^2 allowed at 90% CL by the results of the LSND experiment, taking into account the results of all the other SBL experiments (see Eq.(1.2)).

FIG.2. Upper bounds for the probability of $\nu_\mu \rightarrow \nu_e$ transitions in the K2K experiment. The solid curve is obtained by a numerical analysis of Eq.(3.37) and uses the following experimental input: the 90% CL exclusion plot of the Bugey $\bar{\nu}_e \rightarrow \bar{\nu}_e$ experiment [24], the 90% CL exclusion plots of the BNL E734 [38], BNL E776 [25] and CCFR [39] $\bar{\nu}_\mu \rightarrow \bar{\nu}_e$ experiments and the 90% CL exclusion plots of the CDHS [35] and CCFR [36] $\nu_\mu \rightarrow \nu_\mu$ experiments. The solid curve is the matter-corrected version of the short-dashed curve, which represents the bound (2.13) valid for neutrino oscillations in vacuum (this curve does not need the input of the $\nu_\mu \rightarrow \nu_\mu$ experiments). The long-dashed line represents the bound (3.30) derived from probability conservation and has been evaluated by using the $\bar{\nu}_e \rightarrow \bar{\nu}_e$ data. The dotted curve depicts the ‘‘matter-stable’’ bound (3.26), which needs experimental input from $\bar{\nu}_e \rightarrow \bar{\nu}_e$ and $\nu_\mu \rightarrow \nu_\mu$ transitions. The dash-dotted vertical line represents the expected sensitivity of the LBL accelerator neutrino experiment K2K. The shaded region corresponds to the range of mixing parameters allowed at 90% CL by the results of the LSND experiment, taking into account the results of all the other SBL experiments. The two horizontal borderlines correspond to the limits (1.2) for Δm^2 . The darkly shadowed area represents the allowed region if matter effects are neglected. The left edge of this region is given by the lower bound Eq.(2.14) of LSND on the probability of $\bar{\nu}_\mu \rightarrow \bar{\nu}_e$ transitions. The long-dashed curve constitutes also an upper bound for the probability of $\bar{\nu}_e \rightarrow \bar{\nu}_\tau$ transitions if K2K would use a $\bar{\nu}_e^{(-)}$ beam.

FIG.3. The same as in Fig. 2 but the matter corrections now refer to the MINOS and ICARUS experiments with the dot-dashed and dot-dot-dashed lines as their respective sensitivities.

FIG.4. Upper bounds for the transition probability $1 - P_{\bar{\nu}_e \rightarrow \bar{\nu}_e}^{(\text{LBL})}$ in the Kam-Land experiment. The short dashed curve (see Eq.(2.7)) represents the bound for vacuum oscillations (it is identical with the solid curve in Fig. 1) and is valid also in matter if the solar neutrino problem is explained by the small mixing angle MSW solution. The solid curve represents the bound (3.28) valid in matter with the value of ω_{max} given in Tab. I and it refers to the case of a vacuum oscillation solution of the solar neutrino problem. The dotted, dash-dotted and dash-dot-dotted lines give the upper bounds for $1 - P_{\bar{\nu}_e \rightarrow \bar{\nu}_e}^{(\text{LBL})}$ at different neutrino momenta p in the case of a large mixing angle solution of the solar neutrino problem (see Eq.(2.21)). The long-dashed vertical line depicts the expected sensitivity of the Kam-Land experiment. The shadowed region and the two horizontal solid lines correspond to the range of Δm^2 allowed at 90% CL by the results of the LSND experiment, taking into account the results of all the other SBL experiments (see Eq.(1.2)).

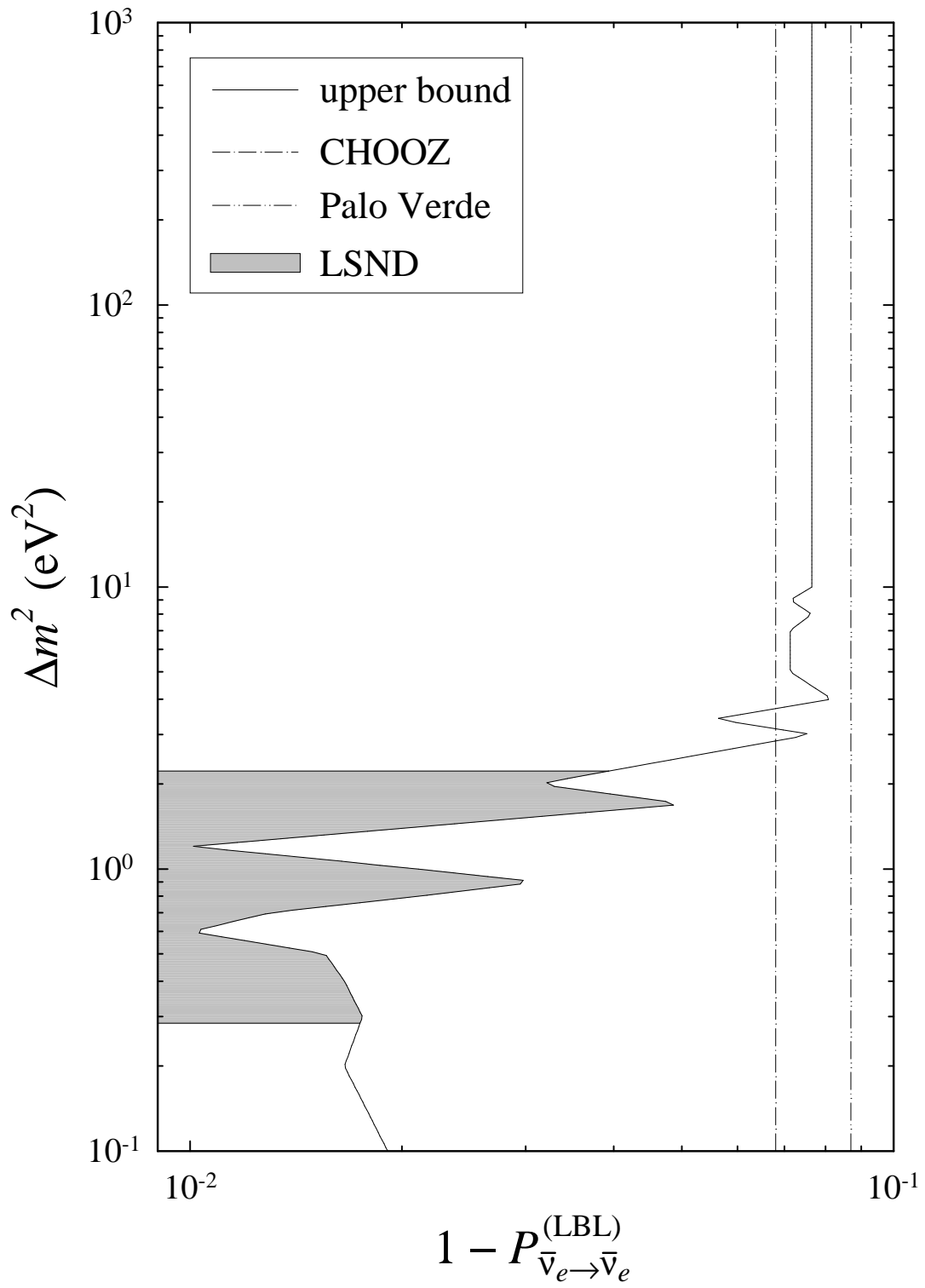


Figure 1

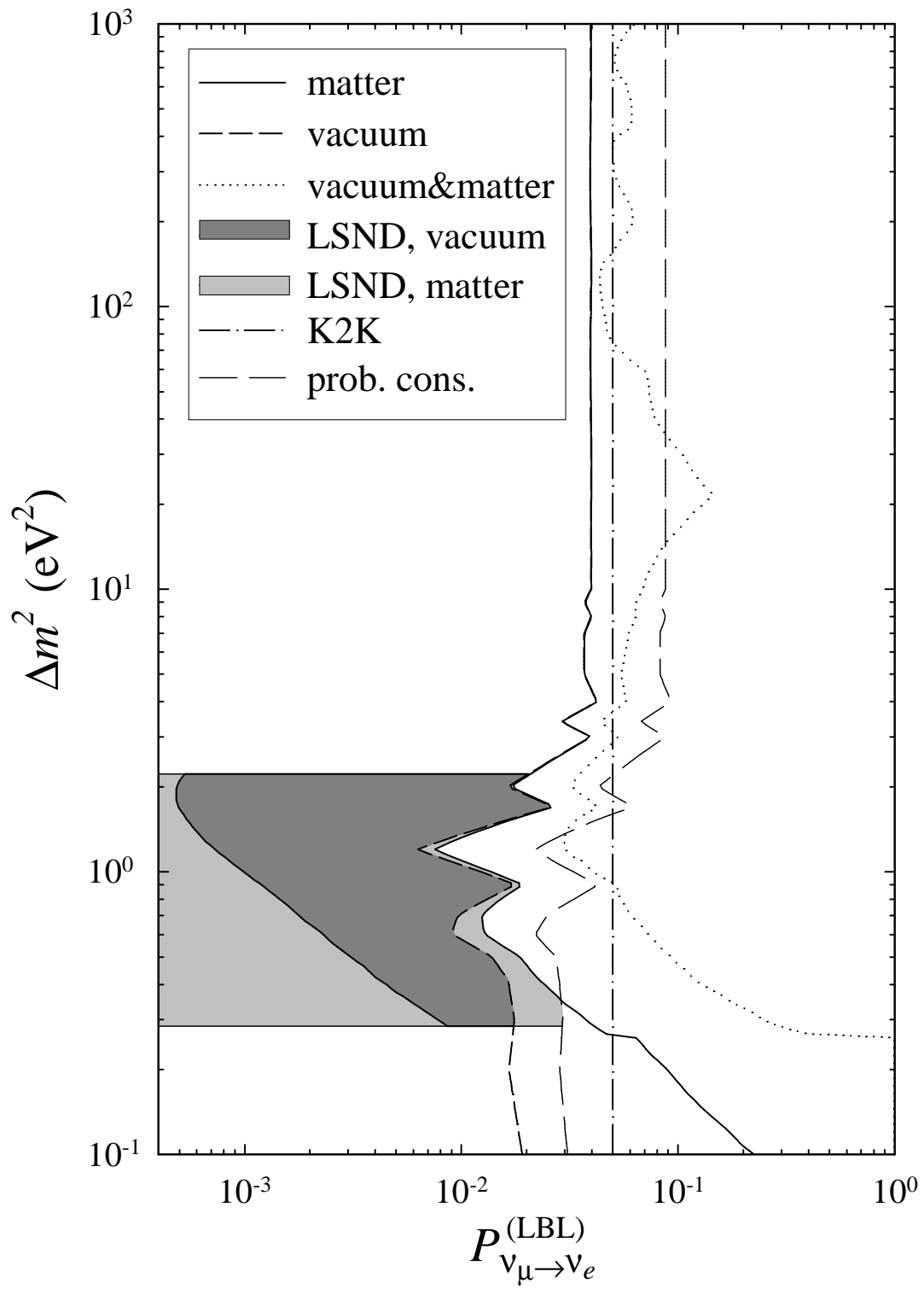


Figure 2

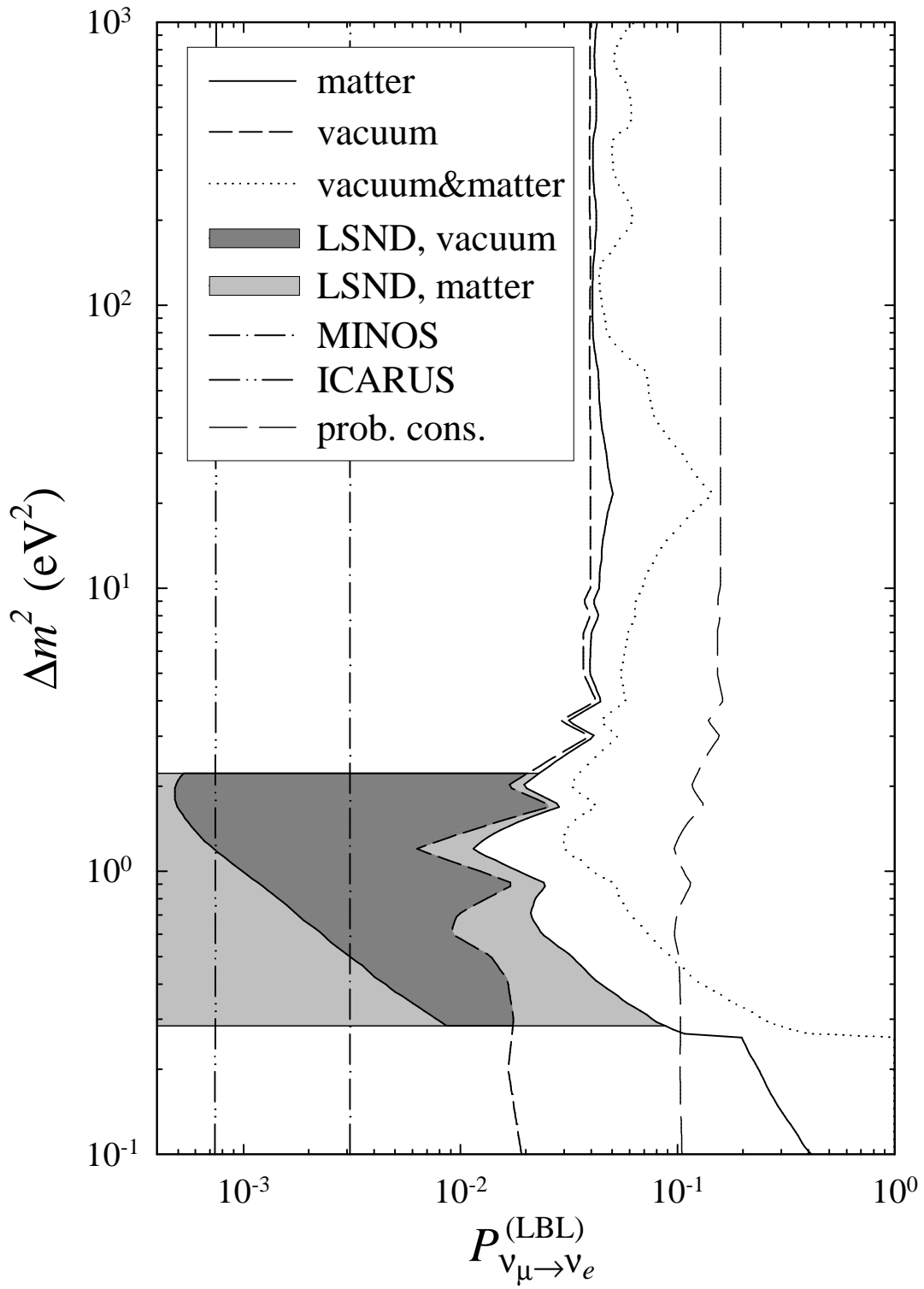


Figure 3

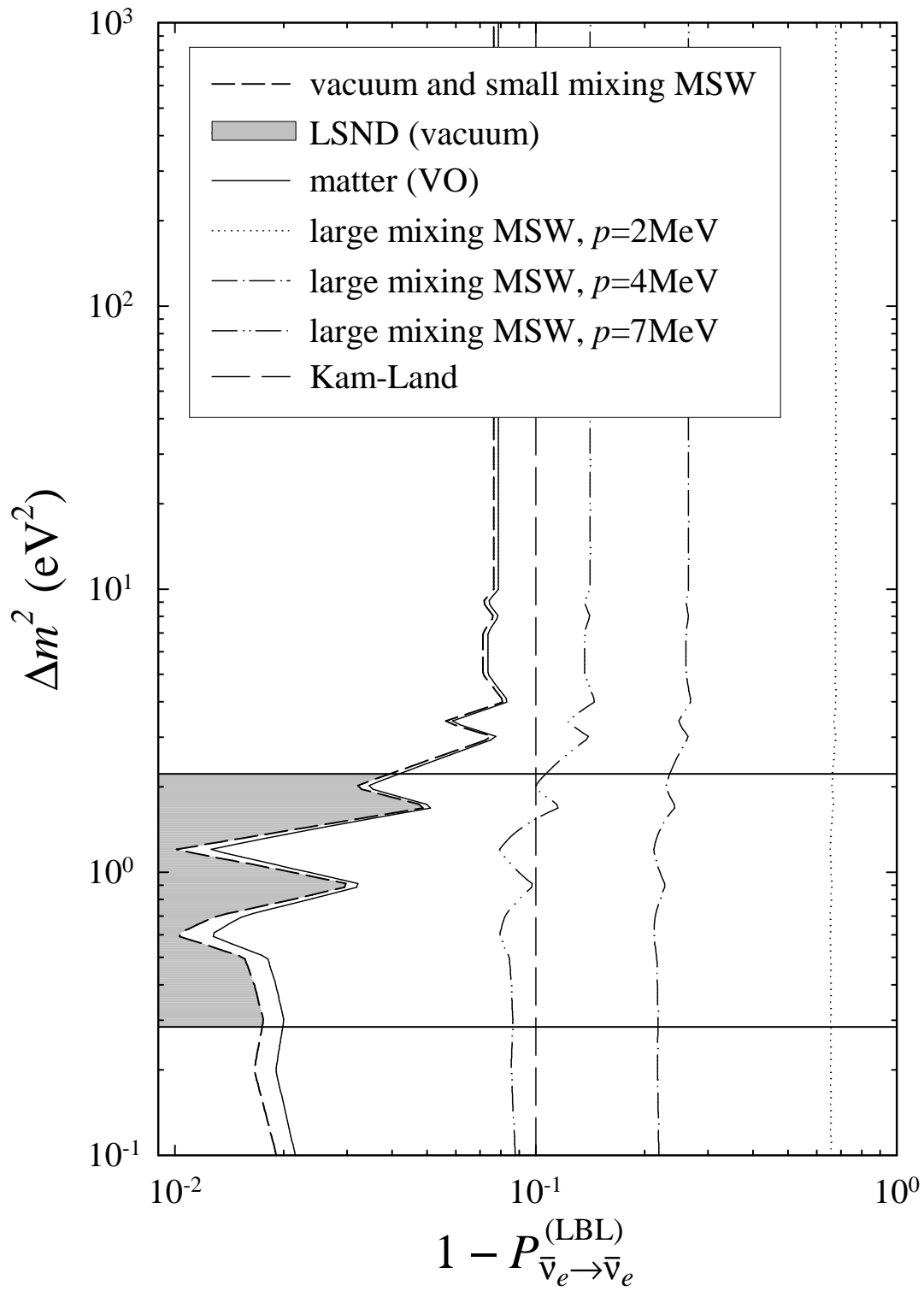


Figure 4